Remote Sensing of Environment 271 (2022) 112908

Contents lists available at ScienceDirect

Remote Sensing of Environment

journal homepage: www.elsevier.com/locate/rse

Intra-annual taxonomic and phenological drivers of spectral variance in grasslands

Rachael Thornley [a,*], France F. Gerard [b], Kevin White [a], Anne Verhoef [a]

[a] University of Reading, Reading, Berkshire, RG6 6AH, UK
[b] UK Centre for Ecology and Hydrology, Wallingford, Oxfordshire, OX10 8BB, UK

ARTICLE INFO

Editor: Marie Weiss

Keywords:
Phenology
Spectral variance
Species diversity
Multi-temporal
Grasslands
Vegetation

ABSTRACT

According to the Spectral Variation Hypothesis (SVH), spectral variance has the potential to predict taxonomic composition in grasslands over time. However, in previous studies the relationship has been found to be unstable. We hypothesise that the diversity of phenological stages is also a driver of spectral variance and could act to confound the species signal. To test this concept, intra-annual repeat spectral and botanical sampling was performed at the quadrat scale at two grassland sites, one displaying high species diversity and the other low species diversity. Six botanical metrics were used, three taxonomy based and three phenology based. Using uni-temporal linear permutation models, we found that the SVH only held at the high diversity site and only for certain metrics and at particular time points. We also tested the seasonal influence of phenological stage dominance, alongside the taxonomic and phenological diversity metrics on spectral variance using linear mixed models. A term of percentage mature leaves, alongside an interaction term of percentage mature leaves and species diversity, explained 15-25% of the model variances, depending on the spectral region used. These results indicate that the dominant canopy phenology stage is a confounding variable when examining the spectral variance-species diversity relationship. We emphasise the challenges that exist in tracking species or phenology-based metrics in grasslands using spectral variance but encourage further research that contextualises spectral variance data within seasonal plant development alongside other canopy structural and leaf traits.

1. Introduction

1.1. Grassland monitoring

An important criterion when assessing field-level grassland condition is the complexity of the plant community, often summarised as the number of taxonomic units co-existing within the sward and their spatial distribution. These surveys are typically targeted at mid growing season when most plants are flowering, a time referred to as peak phenology (Stohlgren, 2006), with few data having been collected outside what is considered to be this 'optimal' window (Magurran, 2007). Plant communities can be dynamic in terms of the number of taxa present at a single time point during a growing season (Mellard et al., 2019; Wang et al., 2016), however, repeat intra-annual botanical surveys are very time-consuming and so little is understood about these community dynamics.

1.2. Spectral variation as a proxy for species diversity

An option to increase our understanding is to utilise remote sensing (Ali et al., 2016; Wachendorf et al., 2017) and in particular hyperspectral reflectance data (Fava et al., 2010; Möckel et al., 2016; Wang and Gamon, 2019). The Spectral Variation Hypothesis (SVH) proposes that the variance in spectral reflectance within a given area can be used as a proxy for plant taxonomic diversity. The concept of reflectance variance as an ecological surrogate was first described by Palmer et al. (2002). Rocchini et al. (2010) provide a review of the concept and the challenges to its implementation. Evidence to support the hypothesis has been gathered at the landscape scale (Hall et al., 2010) using broad-band satellite data products, down to the leaf-level with close-range imaging spectrometers (Wang et al., 2018). In some studies, however, the SVH been found to be unstable (Schmidtlein and Fassnacht, 2017; Torresani et al., 2019) and context dependent (Imran et al., 2021).

Convergent optical properties of photosynthetically active material

* Corresponding author at: University of Reading, Reading, Berkshire, RG6 6AH, UK.
E-mail addresses: r.h.thornley@pgr.reading.ac.uk (R. Thornley), ffg@ceh.ac.uk (F.F. Gerard), k.h.white@reading.ac.uk (K. White), a.verhoef@reading.ac.uk (A. Verhoef).

https://doi.org/10.1016/j.rse.2022.112908
Received 24 March 2021; Received in revised form 8 January 2022; Accepted 12 January 2022
Available online 24 January 2022

alongside the impact of environmental drivers, such as water availability, may prove obstacles to species differentiation (Asner et al., 2009; Ollinger, 2011). Furthermore, spectral distance between species may be affected more by functional variation rather than by the number of taxonomic units (Schweiger et al., 2018). This perspective is intrinsic to the 'optical type' theory (Ustin and Gamon, 2010), where, in the context of high spatial resolution reflectance data, 'diversity' can be framed as a product of leaf traits at the individual level (Leaf Mass Area, Nitrogen, Chlorophyll, Carotenoids, Lignin) rather than taxonomic variation (Ma et al., 2020).

1.3. Measures of spectral variance

One of the complications in assessing the SVH and prior findings in this field, is that measures of spectral variance are calculated in different ways. Sophisticated approaches have been employed to deal with the multi-variate data sets produced from hyperspectral data sensors, for example, the 'Spectral Angle Mapper' (Gholizadeh et al., 2018), k-means clustering (Rocchini et al., 2005) and Partial Least Squares regression (Möckel et al., 2016; Polley et al., 2019). It is arguable, however, that descriptive statistical approaches, such as taking dispersions around the mean value for a single wavelength or index value, are more useful at this stage to evaluate the hypothesis (Torresani et al., 2019; Wang et al., 2018) as they allow the strength of the relationship to be more effectively compared between study findings. The coefficient of variation (CoV) is an often-used metric when dealing with hyperspectral data (Aragón et al., 2011; Blanco-Sacristán et al., 2019; Lucas and Carter, 2008; Wang et al., 2018) as it normalises the dispersion against the mean reflectance for each wavelength, thus accounting for the differences in magnitude between spectral regions.

1.4. The performance of the SVH over time

Another obstacle is that the relationship between spectral variance and taxonomic diversity when examined over time has been shown to be inconsistent (Schmidtlein and Fassnacht (2017)). Inter-annual studies with similar sampling dates in temperate systems (Gholizadeh et al., 2020) suggest this inconsistency is not merely a product of 'time of year' but may be due to a complex relationship between reflectance and seasonally dynamic leaf and canopy traits (Feilhauer and Schmidtlein, 2011; Feilhauer et al., 2017). High spatial resolution hyperspectral data, to our knowledge, has been collected on multiple dates in grasslands for only a couple of studies (Feilhauer and Schmidtlein, 2011; Gholizadeh et al., 2020), both of which reported varying relationships over time between taxonomic diversity and spectral reflectance. These observations could be due to the dynamic nature of grassland canopies, in terms of their responses to rainfall and management (Li et al., 2013) and phenological variability (Ustin and Gamon, 2010).

1.5. The impact of phenological stage on the spectral variation

Hyperspectral reflectance data are usually collected at peak biomass or growth when assessing taxonomic diversity, and there is good theoretical basis for this decision. At these times, grassland canopies are generally less affected by dead plant tissue and exposed soil, which are significant additional sources of spectral variation (Asner, 1998). When these sources are minimised, leaf intracellular structure and chemical traits drive variation in leaf reflectance (Ollinger, 2011; Ustin et al., 2009) and it is this variation that has been shown to be strongly correlated with the species present (Asner and Martin, 2011, 2016). In addition, leaf traits and so reflectance, and derived vegetation indices, alter with leaf age (Chavana-Bryant et al., 2017) which, if not accounted for, could be confounded with, among others, a taxonomic signal. On the other hand, the effect of leaf age and plant life cycle stage on reflectance could be exploited when the aim is to map single species or functional types. For example, in temperate deciduous woodlands, species specific timing of leaf emergence and senescence, accompanied with species specific leaf colouring, have been instrumental in distinguishing between tree species (Fassnacht et al., 2016; Hill et al., 2010; Voss and Sugumaran, 2008).

The spatial scale of data acquisition is highly significant when assessing the SVH (Gamon et al., 2019). At the leaf level, phenological stage affects reflectance through the process of leaf maturation (the development of palisade and spongy mesophyll and increase in chlorophyll cell number) (Noda et al., 2021), followed by senescence (reallocation of resources away from the leaf to over-wintering or reproductive structures). At the canopy scale, the quantity and developmental stage of leaves affect reflectance through increases in parameters such as leaf area index (LAI) and total canopy chlorophyll (Jacquemoud et al., 2009). Non-leaf plant architecture (buds, flowers, seeds) will also influence reflectance as these parts of the plant are generally not photosynthesising (Asner, 1998).

The number of differing phenological stages present will therefore be an additional driver of spectral variation alongside taxonomic diversity. The extent to which individuals within plant communities exhibit phenological stages at simultaneous or staged phases is known as phenological synchrony or asynchrony (Rathcke and Lacey, 1985; Forrest and Miller-Rushing, 2010) and the number of co-occurring phenological stages can be understood as phenological diversity (Lasky et al., 2016; Ramos et al., 2014). These properties may, however, be difficult to estimate as they are likely to vary between years and within a growing season (Mazer et al., 2013; Tansey et al., 2017) due to individual-based responses to environmental conditions (Wolkovich et al., 2014).

1.6. Study aims

This study uses intra-annual repeat taxonomic and phenological observations alongside the variance of high-resolution spectral reflectance data collected at two grassland sites, with differing levels of species diversity, soil type and management regime, to test the following:

1) The temporal stability of the SVH across a growing season in relation to plant taxonomic metrics and to determine the best time of year for biodiversity surveys using this method.
2) The extent to which the phenological diversity of the canopy drives spectral variance.
3) The relative impact of phenological and taxonomic diversity and phenological stage dominance on spectral variance across the growing season.

2. Methods

2.1. Grassland site description and sampling campaign overview

Two sites in the south east of England were used for the collection of remote sensing and botanical data. The first site is Dawcombe nature reserve, Betchworth, Surrey, UK (51.259, −0.261). It is an example of medium quality chalk grassland situated on the scarp slope of the North Downs and is managed for biodiversity conservation. From hereon, this site will be referred to as 'Dawcombe'. The second site is a long-term experimental grassland managed by Imperial College London and called 'Nash's Field' located at Silwood Park, Sunningdale, Berkshire, UK (51.413, −0.645). It is composed of acid grassland plots that have undergone varying soil nutrient and grazing treatments (Crawley et al., 2005). The range of treatments have created a site with high levels of community variation within a small area. This site will be referred to as 'Silwood'. Both sites undergo annual late summer or winter biomass removal through mowing and grazing but are not managed during the spring and summer months when the sampling was undertaken. However, they are subject to some low-level grazing throughout the year by wild herbivores (deer and rabbits) and invertebrates. We selected the

sites for their strong gradients of community composition. They are also grasslands where plant species undergo their reproductive cycles without significant interruption, unlike in many agricultural grasslands where high grazing pressures can occur throughout the year.

Twenty 50 × 50 cm (0.25m^2) quadrats sub-divided into twenty-five 10 × 10 cm subquadrats, using a botanical grid as a guide, were measured over the 2019 growing season. Ten of these were situated at Dawcombe and ten at Silwood (see Fig. 1). Quadrats were used as they represent the most common approach to monitoring vegetation in grasslands. At Dawcombe, quadrat locations were randomly chosen along a slope gradient, intended to capture maximum variation in the plant community, and were simply labelled 1–10. At Silwood, the quadrats were chosen to represent a range of nutrient and grazing applications, to the same aim. They were labelled to reflect the experimental plot (L), whether they were subject to grazing (UF = unfenced) or not (F = fenced) and the nutrient treatment (N = nitrogen, K = potassium, P = phosphate, All = all nutrients, None = control). The quadrats were marked with pegs and geolocated to sub-cm accuracy by use of a differential GPS so the same areas could be revisited. The botanical sampling grid was painted matt black to avoid interference with the reflectance observations. Botanical observations were made at six time points at Silwood and ten at Dawcombe. Hyperspectral sampling events totalled five at Silwood and seven at Dawcombe. Details of botanical and spectral sampling are to follow.

2.2. Plant community metrics

We calculated two sets of metrics, which are listed with their respective equations in Table 1. The first set is based on *taxonomic* units and metrics were calculated per time point per quadrat. The second set is designed to evaluate the impact of plant phenological stage on spectral diversity. These metrics are based on *phenological* observations associated with the recorded taxa and were also calculated per time point per quadrat.

2.2.1. Taxonomic metrics

Plant taxonomic complexity can be described and summarised by using a range of metrics, each of which present a different aspect of, or approach to, diversity measurement (Magurran and McGill, 2011; Morris et al., 2014). The following three metrics were calculated (Table 1): 'species richness', which is a count of species occurrence and is the basic measure in biodiversity assessment; the 'Simpson evenness index', also known as relative abundance (Smith and Wilson, 1996) which describes the dominance distribution of the species present; and the 'Simpson diversity index', a composite measure which incorporates both richness and evenness. Visual estimations of percent cover per species, are often used in botanical assessments, but this measure is very subjective, especially in more complex species-rich quadrats. So, instead, the proportion of sub-quadrats in which the species occurred was used to calculate relative abundance and subsequently derive the Simpson's diversity and Simpson's evenness indices.

Because proximal remote sensing instruments are generally set to

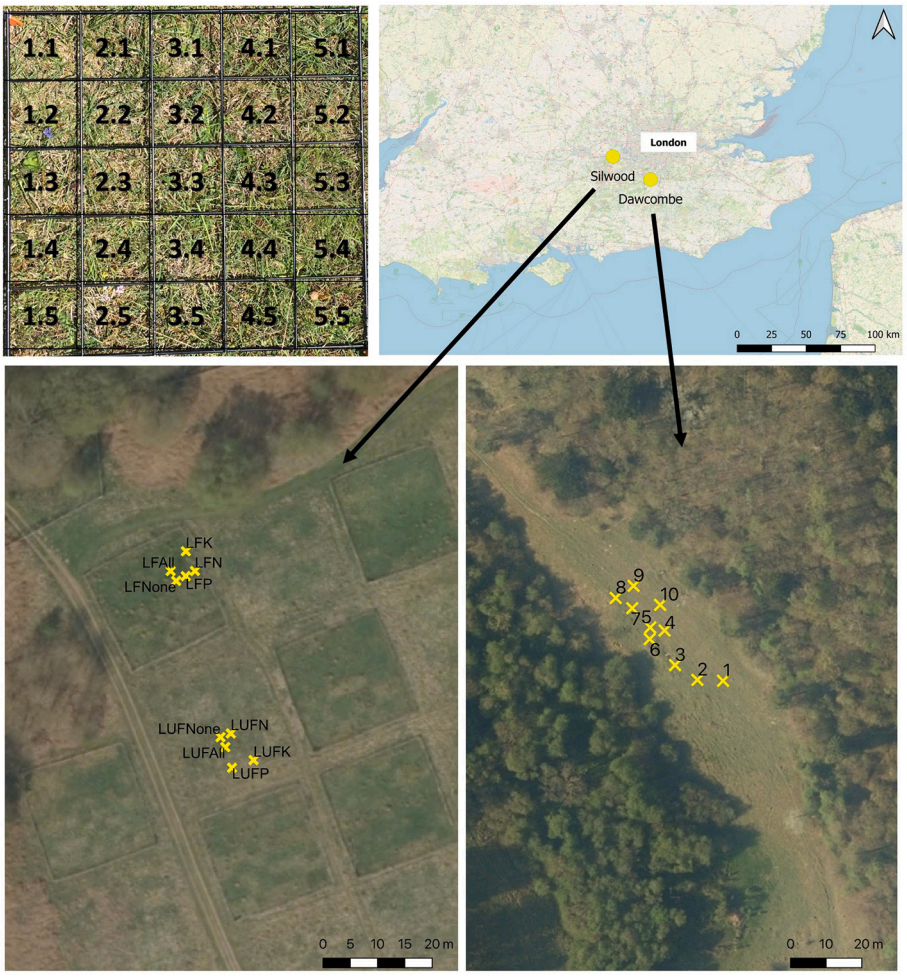

Fig. 1. The sampling sites and the quadrat locations at Silwood and Dawcombe. Top left: the sampling grid used to acquire both spectral and botanical samples for each of the 20 quadrats at each time point.

Table 1
Definitions of the taxonomic and phenological metrics used in this study.

Name of Metric	Description	Category	Equation
Species Richness (S)	The total number of species observed for each time point (t)	Taxonomic	S_t
Species Diversity (Simpson's diversity inverse or reciprocal) (D)	The inverse of the probability that two species drawn from the same sample will belong to the same species. Index ranges from 1 to infinity, where 1 represents a community with a single species and the higher the number the more complex the community.	Taxonomic	$D_t = \frac{1}{\sum_{i_t}^{S_t}\left(\frac{N_{it}}{N_t}\right)^2}$ Where: N is the total species abundance; N_i is the abundance of species i; t is time point t
Species Evenness (Simpson's Evenness) (E)	Describes the distribution of individuals among classes and is therefore a measure of relative abundance. E is expressed as a proportion of the maximum value which D could assume if individuals in the community were completely evenly distributed (which equals S). The metric takes a value between 0 and 1 where 1 is complete evenness.	Taxonomic	$E_t = \frac{D_t}{S_t}$
Phenological Richness (P)	The number of phenological stages observed for each time point (t)	Phenology	P_t
Phenological Diversity (PhenD)	Index ranges from 1 to infinity, where 1 represents a community with a single phenological stage present and higher values indicate a greater number of phenological classes and a more complex distribution of classes among species.	Phenology	$PhenD_t = \frac{1}{\sum_{i_t}^{P_t}\left(\frac{M_{it}}{M_t}\right)^2}$ Where M is the total number of phenology stages observed and M_i is the total number of phenology stages observed for species i. t is time point t
Phenological Evenness (PhenE)	As definition for E *but for phenological stage*	Phenology	$PhenE_t = \frac{Phen\ D_t}{P_t}$

nadir viewing and so are limited to sensing the top part of canopies, only species within the quadrat that were observed when looking directly down were considered.

2.2.2. Phenology metrics

Firstly, for each taxonomic unit observed in in the quadrat, an observation of phenological stage was made according to the definitions in Table 2. Some species displayed multiple stages at a single time point. The number of observations in each phenological category were then summed and weighted to produce a measure of phenology stage dominance for each quadrat at each time point.

Measures are available that describe the timing of plant phenology stages, such as frequency, regularity, amplitude, synchrony and duration (Newstrom et al., 1994; Denny et al., 2014). However, to evaluate the impact of plant phenological stage on spectral variance we required metrics that capture the phenology stage diversity observed at any moment in time. As far as we are aware, these do not exist. We therefore adopted the above taxonomic metrics to produce the following phenological metrics: 'phenological richness', the number of different phenology stages present at a given time in a given quadrat'; phenological evenness', a measure of the relative abundance of phenology stages present; and 'phenological diversity' which was designed to reflect the diversity of phenology stages present at any moment in time within a quadrat, as a product of the species richness and abundance. For full definitions of the metrics and the calculations used to produce them see Table 1.

Table 2
Descriptions of the phenology stages used to calculate the phenological diversity metrics.

Phenology stage code	Stage name	Stage description
SEN(1)	Senescent	Plant material in senescence (brown, lacking in chlorophyll) when quadrat was first examined in the spring (principally from last years' growth season).
YOU(2)	Young	Leaf material is thin/downy – displays colours (bright green) not in line with those expected from mature leaves.
MAT(3)	Mature	Leaf material is thickened / some cases waxy – displays colours in line with those expected from mature leaves
BUD(4)	Budding flowers	Plant has the beginnings of reproductive organs - flower buds for broadleaved herbs, or sheathed heads for grasses
FLO(5)	Flowering	Plant is in flower; flower heads emerged
SEE(6)	Seeding	Plant has seeds or seed encapsulating organs visible
SEN(7)	Senescent	The current growth season's plant material in senescence (brown or red/brown discoloured leaves).

2.3. Spectral data capture and calculation of spectral variance

The Coefficient of Variance (CoV) from hyperspectral reflectance observations was selected as the spectral variance metric. The next sections outline the in-situ instrument setup and hyperspectral data pre-processing steps taken to ensure a robust dataset for reliable derivation of reflectance CoV.

2.3.1. Hyperspectral field radiometry setup

Hyperspectral reflectance measurements (350 nm – 2500 nm) were collected for each sub-quadrat (25) of each quadrat (20). We used two SVC non-imaging spectrometers (SVC HR2024i spectroradiometers, Spectra Vista Corporation, USA) in a Dual Field Of View (DFOV) mode (Maclellan, 2017; Punalekar et al., 2018), to simultaneously record irradiance and reflected radiance. This approach is recommended when data is collected under fluctuating illumination conditions (which is often the case in the UK) and is expected to deliver more accurate observations, which are particularly important when, as in most vegetation studies, spectral distance between target classes is small. Before target sampling began, both spectrometers were mounted on tripods pointing at their respective Spectralon panels and reference readings were taken concurrently. The instrument measuring down-welling radiation was then set to timed-mode while the instrument measuring upwelling radiation was used on a boom held at nadir 70 cm above the grassland canopy, resulting in a sample spot size of 10 cm. Each grassland quadrat measured 50 × 50 cm and was subdivided into twenty-five 10 × 10 cm sub-quadrats using as a guide, the same matt black grid that was used in the botanical sampling. For each sub-quadrat one reading was taken. The target spots were intended to be non-overlapping but spatially correlated in order to emulate the effect of pixels from an imaging sensor. All measurements were taken between the hours of 10 am and 3 pm local time (BST). Twenty-five measurements were taken of each

quadrat at each time point resulting in 250 measurements per sampling date for each site, totalling 3000 spectral samples.

2.3.2. Hyperspectral data pre-processing

Pre-processing of the spectrometry data involved calibration of each sub-quadrats' reflected radiance spectrum against its respective Spectralon white reference panel spectrum to produce reflectance. Parts of the spectrum affected by water absorption and scattering were removed (339–399 nm, 1900–2051 nm, 2450–2519 nm) and a Savitzky-Golay smoothing filter was applied. The spectrum was binned by 10 nm increments. Smoothing and binning was carried out with the package HSDAR (Lehnert et al., 2019) in R (R Core Team, 2021).

Spectrometry data can suffer from erroneous measurements caused by slight changes in viewing angle and subject illumination (Wehrens, 2011). It is vital to ensure that the inclusion of these measurements is minimalised as we are dealing here with variance measures from a mean or a centroid value. A common practice is to carry out repeat measures of the same target and take an average. Due to the number of measurements required per day this process was not feasible. Instead, thorough data cleaning and pre-processing was carried out to identify the erroneous readings. Two principal sources of measurement error were considered; 1) time stamp mismatch between the two spectrometers (one measuring the quadrats, the other the white reference panel), especially in rapidly changing conditions and 2) changes in reflectance caused by variations in viewing and sun angle. To minimise these sources of error, we used 'Robust Principal Component Analysis' (ROBPCA) (Hubert et al., 2005; Hubert, 2020) which was applied to the spectra grouped by time-point and quadrat (amounting to 120 data sets). Outliers are computed using 'projection pursuit' techniques and the Minimum Covariance Determinant (MCD) method (Hubert and Debruyne, 2010). The ROBPCA approach can be used to compute PC scores that are outlier resistant, but also to detect the outliers themselves. The level of data cleaning changed with the α parameter (0.5–0.9); lower values indicate more 'robust' outlier detection, with more samples being removed from the analysis. Data sets produced with five values of α (0.5, 0.6, 0.7, 0.8 and 0.9) were used to help assess the stability of the model fits for the uni-temporal data sets (Section 2.5.1). For the rest of the analysis, we used the ROBPCA corrected data with an α value of 0.8 resulting in a total sample size of 2561 spectra. For sample sizes, the sampling dates and their corresponding day of year (DoY) see Table 3.

2.3.3. Coefficient of variation

The coefficient of variation (CoV) was used as the spectral diversity metric and was calculated for each waveband *i* as follows:

$$CoV_i\ (\%) = \frac{\sigma_i}{\mu_i}\ x\ 100 \quad (1)$$

where μ_i equals the mean reflectance of the 25 subplots and σ_i equals the standard deviation. Wang et al., 2018 used the mean of the band specific CoV values across spectral regions as a summary measure of hyperspectral variance and found strong positive correlations with taxonomic diversity metrics. Here we follow this method in order to compare findings. Firstly, the band specific measures of CoV were averaged across the full visible to short wave infra-red spectrum and then, secondly, across three spectral regions; the visible (400–699 nm), the near infra-red (700–1299 nm) and the short wave infra-red (1300–2519 nm). These averages are referred to as 'mean-CoV', 'vis-mean-CoV', 'NIR-mean-CoV' and 'SWIR-mean-CoV', respectively. Although the exact values of these regional cut-off points are somewhat arbitrary, spectral variation within these three chosen spectral regions (visible, NIR and SWIR) has been shown, through use of radiative transfer models and global sensitivity analysis, to be driven by different leaf or canopy traits (Li and Wang, 2011; Xiao et al., 2014). At the leaf level, use of the PROSPECT model (Jacquemoud and Baret, 1990) shows that global spectral variation is dominated by variation in chlorophyll concentration in the visible region (400 nm – 699 nm) and the leaf structural parameter (N) in the NIR (700–1299 nm). Although the influence of N is still relevant at certain spectral sub-regions beyond 1300 nm, equivalent water thickness (Cw) becomes the principal contributor to spectral variance throughout the SWIR region (1300– 2500 nm). Similarly, at the canopy scale, the PROSAIL model (Jacquemoud et al., 2009) shows that these spectral regions retain their discrete importance. Variation in reflectance in the visible region is driven by chlorophyll content and by water throughout the SWIR. In contrast to the leaf level, at this scale, spectral variation in the NIR is mainly driven by dry matter content (Cm) and leaf area index (LAI). We hypothesise that, during the growing season, different leaf and canopy traits will be dominant in driving spectral variance and summarising data by these regions will help with interpretation of results.

Table 3
Sample sizes and dates for the hyperspectral data set.

Site	Date	Day of Year	Time point	Spectrometer sample size(n=)	
				All data	ROBPCA screen
Dawcombe	18th April 2019	108	1	250	216
	1st May 2019	121	2	250	215
	16th May 2019	136	3	250	209
	31st May 2019	151	4	N/A	N/A
	11th June 2019	162	5	N/A	N/A
	27th June 2019	178	6	N/A	N/A
	13th July 2019	194	7	250	215
	24th July 2019	205	8	250	217
	8th August 2019	220	9	250	211
	20th August 2019	232	10	250	213
Silwood	29th April 2019	119	1	250	210
	21st May 2019	141	2	250	217
	5th June 2019	156	3	250	218
	20th June 2019	171	4	N/A	N/A
	12th July 2019	193	5	250	210
	29th July 2019	210	6	250	210

2.4. Satellite NDVI to contextualise findings

A time-series of satellite derived NDVI values obtained from the Sentinel-2 mission at 10 m spatial resolution was used to contextualise the findings of the field observations in terms of the main growing season periods: green-up, peak biomass and senescence (Fig. 2). For each available time-point, cloud free MSI pixels corresponding with site quadrats locations were extracted and a site-specific mean NDVI (and standard error) was calculated. Seven pixels over 31 dates were used to construct the time-series for Dawcombe and five pixels over 19 dates for Silwood.

The NDVI time-series were divided into three phenology stages, which we call "Pre-NDVI max" (representing 'green-up' of the site vegetation), "NDVI max" (the plateaux of maximum NDVI which we assume to coincide with the vegetation being at maximum growth stage) and "Post-NDVI max" (where vegetation begins to senescence). The period of peak growth (NDVI max) corresponded to 25 days either side of the highest NDVI value, although this value was more difficult to ascertain at Silwood, as the site exhibited cloudy conditions at this time

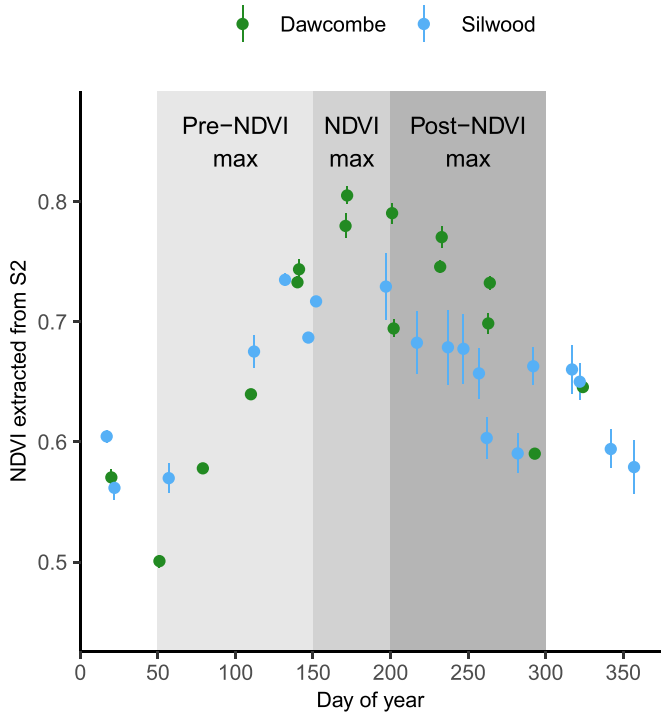

Fig. 2. The three phenology stages (Pre-NDVI max, NDVI max and post-NDVI max) derived from Sentinel-2 MSI NDVI time-series for two grassland sites.

of year. Pre-NDVI max covers the months of March, April and May (DoY 50 to 150), NDVI max covers June and the first half of July (DoY 150 to 200) and Post-NDVI max covers late July, August and September (DoY 200 to 300).

2.5. Statistical analysis of spectral variance and taxonomic and phenological metrics

The key aims of this study are to test the temporal stability of the SVH in relation to taxonomic metrics and to assess the extent to which phenological diversity drives spectral variance. In order to test these hypotheses two types of modelling were carried out. The first consisted of simple linear models which assessed the strength of the relationship between spectral variance and the three taxon and three phenology based metrics at each sampling event at each site. The second utilised mixed models to evaluate the consistency of these same relationships over all sampling points and across both sites.

We also used mixed modelling to investigate the third aim of the work which was to assess the relative impact of taxonomic and phenological diversity, alongside phenological stage dominance on spectral variance over all sampling points.

2.5.1. Simple linear models

Simple linear models were used to test the relationship between each narrow band value (the hyperspectral approach), as well as mean-CoV, vis-mean-CoV, NIR- mean-CoV and SWIR-mean-CoV, (the spectral regions approach) and the three species-based and three phenology-based diversity measures. For the spectral regions models, 288 uni-temporal model runs were carried out (Dawcombe: 7 time-points x 6 diversity metrics x 4 spectral regions =168 and Silwood: 5 time-points x 6 diversity metrics x 4 spectral regions = 120). Our data sets are small, when considered for each time point and site, so a permutation modelling approach was applied (LaFleur and Greevy, 2009), where *p* values for each linear model are assessed for stability using imputation, and the resulting adjusted r^2 values are reported.

2.5.2. Linear mixed models

One of the challenges associated with the data set collected is its structure, which includes temporal and spatial auto-correlation. Each quadrat was revisited several times so within-quadrat samples could be more similar to each other than to the data from other quadrats. It is also possible that samples taken at similar times of year will be more similar to each other. With this in mind, all data were modelled using a mixed model (Zuur et al., 2009), where the fixed effect is the taxonomic or phenological metric and the random effects, the quadrat and sampling time point (Pinheiro and Bates, 2000).

The package *lme4* (Bates et al., 2015) in R was used for the mixed model analysis. The model random effects structure was determined following the procedure outlined in Barr et al. (2013). The model fitting was performed using restricted maximum likelihood (REML) and the most complex random structure that would converge, used sampling event (day of year) and quadrat as random effects, producing an intercept only model with two random terms. Site was added as a fixed effect, because it only has two levels (the recommended minimum number of levels in a random effect is five (Zuur et al., 2009)). Examination of model residuals displayed heteroscedasticity, so spectral variance was converted to the natural log. This brought the residuals into an acceptable distribution. Application to the model residuals of a first order autocorrelation function revealed no significant temporal autocorrelation (Mitchell et al., 2020).

We also used mixed modelling to investigate the sources of spectral variance over time and used spectral variance as the response variable. Before modelling, all predictor variables are scaled from −1 to +1 and centred to allow interaction effects to be suitably assessed. The maximal model, containing the same random effects structure as in the first modelling stage, was fitted by Maximum Likelihood (ML) with all six of the taxonomic and phenology-based community variables and the percentage canopy stages as predictors with interaction terms included. The most parsimonious model, assessed using Akaike Information Criterion and Bayesian Information Criterion, included the terms % Mature leaves (MAT(3)) and species diversity and a term of their interaction.

For both stages of mixed modelling, reported coefficients, confidence intervals and *p*-values for fixed effects were obtained by fitting the models using Restricted Maximum Likelihood (REML) and by use of the Swatterwaite post-hoc test. Two pseudo r^2 were calculated to assist with the evaluation of the models: the marginal r^2, which is the fixed effects variance divided by the total variance (fixed + random + residual) and the conditional r^2, which is the fixed and random effects variance divided by the total variance. The marginal r^2 indicates the percentage of the total model variance explained by the fixed effects and the conditional r^2 indicates how much of the model variance is explained by the complete model (Nakagawa and Schielzeth, 2013). These values enable assessment of the relative impact of the spatial (quadrat) and temporal (sampling time) grouping variables and the fixed-effect predictor variables.

3. Results

3.1. Plant taxonomic and phenological diversity between sites and over time

The two sites were very distinct in terms of their species and phenology-based community composition (Fig. 3a). Throughout the season, relatively speaking, species richness is low to medium at Silwood (1–10 species) and medium to high at Dawcombe (9–24 species). Dawcombe shows very high levels of quadrat evenness (0.4–0.6) in all quadrats at all times, meaning there is no single dominant species. Silwood displays a range of quadrat evenness from 1.0 (only one species present – so completely even) to levels comparable with Dawcombe for more uneven quadrats (0.4).

In terms of phenological richness, Dawcombe shows higher values, partly reflecting the fact that the site has more species, so is more likely

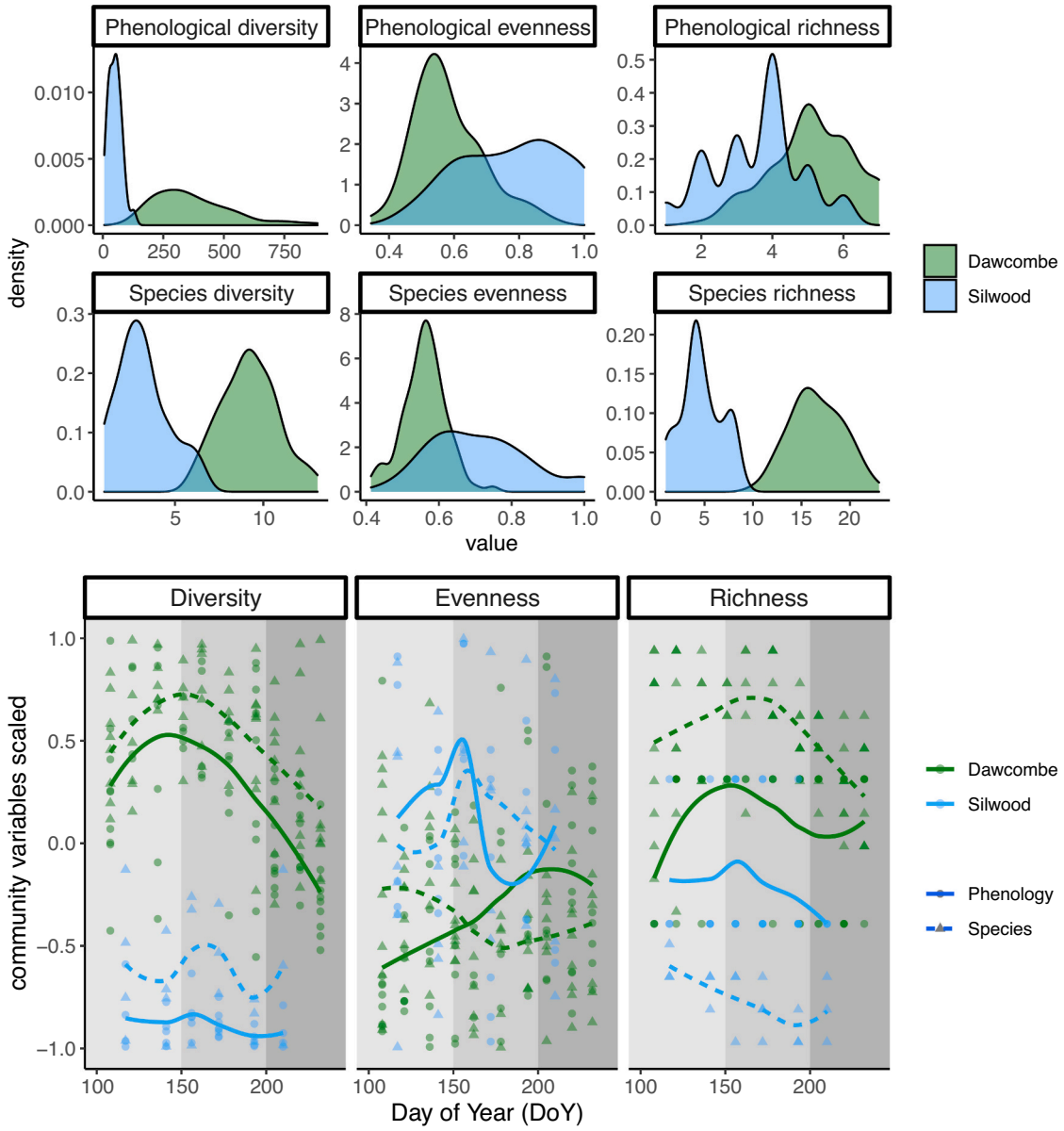

Fig. 3. a (top): Density distributions of the community metrics across the two sites for all times. b: (bottom): Community metrics over time at the two sites. All metrics have been scaled so they can be displayed together and the inter-site differences can be emphasised. A lowess smoother has been applied to emphasise any seasonal data trends.

to have many phenological stages occurring at one time. Results for phenological evenness concur with species evenness, with Silwood having more phenologically homogenous swards compared to Dawcombe. All quadrats at Silwood have low phenological diversity, whereas at Dawcombe there is a large spread in the values of this metric with some quadrats displaying different species' specific phenological states simultaneously.

In terms of seasonal patterns (Fig. 3b), at Dawcombe phenological richness and diversity follow species richness and diversity, with a sharp build up at pre-NDVI max stage followed by a peak at around DoY 150, and then a decline into post-NDVI max. Both species and phenology diversity metrics at Silwood, the species poor site, peak slightly later than at Dawcombe, and less strongly, coinciding more with NDVI-max. These results suggest that if we want to capture the full extent of species and phenological diversity we should sample just before and during NDVI-max. We speculate that both spring and summer emerging species are occurring simultaneously at this time, thus maximising measures of both species and phenological diversity.

When comparing the community metrics for each site using pair-wise correlation (Fig. 4), high intra-site positive correlation between species richness and species diversity can be observed (Pearson's correlation coefficient of 0.83 at Dawcombe and 0.93 at Silwood). The strength of the pairwise correlations between the two types of community metrics (species and phenology based) is generally greater at Silwood than at Dawcombe. This result indicates that at the species poor site (Silwood), phenological traits of the community over the whole season are more closely aligned to species community traits and in contrast, at the more species rich site (Dawcombe), phenological and species traits are more divergent.

Phenological stage dominance was determined by use of the seven phenological stage definitions and weighted percentages of total canopy coverage per stage per quadrat were calculated (Fig. 5). YOU(2) (young material) dominated the swards at both sites in early spring sampling (DoY 108 and 121 at Dawcombe and DoY 119 at Silwood). By DoY 156 at Silwood no new material was emerging, except in very small amounts in three quadrats (LUFN and LUFNone and LUFP). In contrast, at

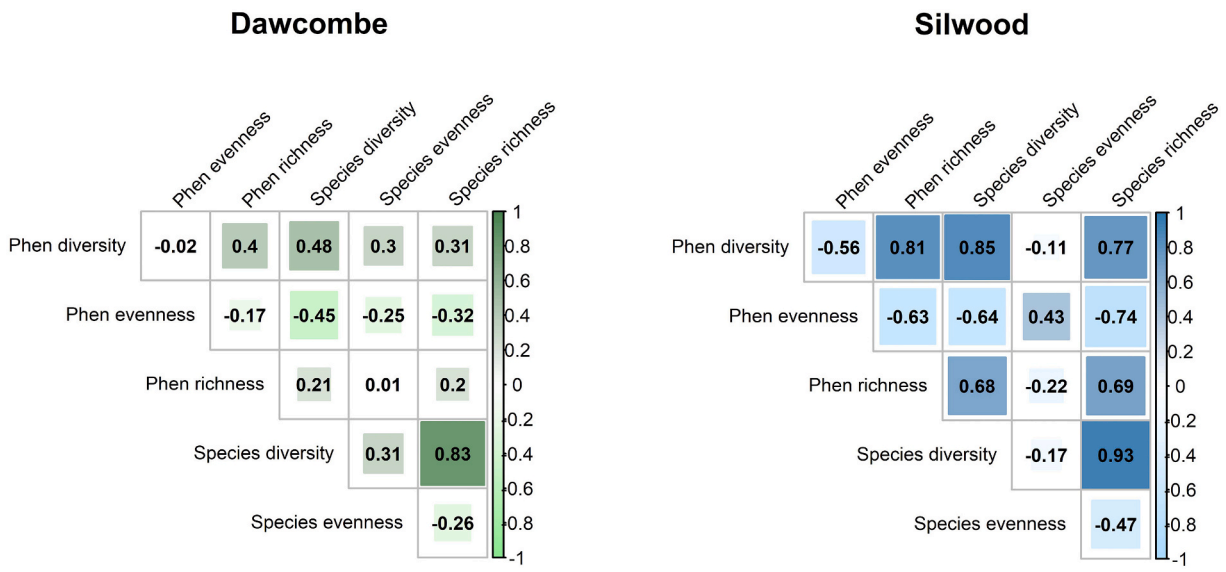

Fig. 4. Correlation heat map of the taxonomic (Species diversity, evenness and richness) and phenology (Phenological diversity, evenness and richness) metrics over all sampling times. Pearson's correlation coefficients are shown. Light colours indicate a negative correlation; dark colours a positive correlation.

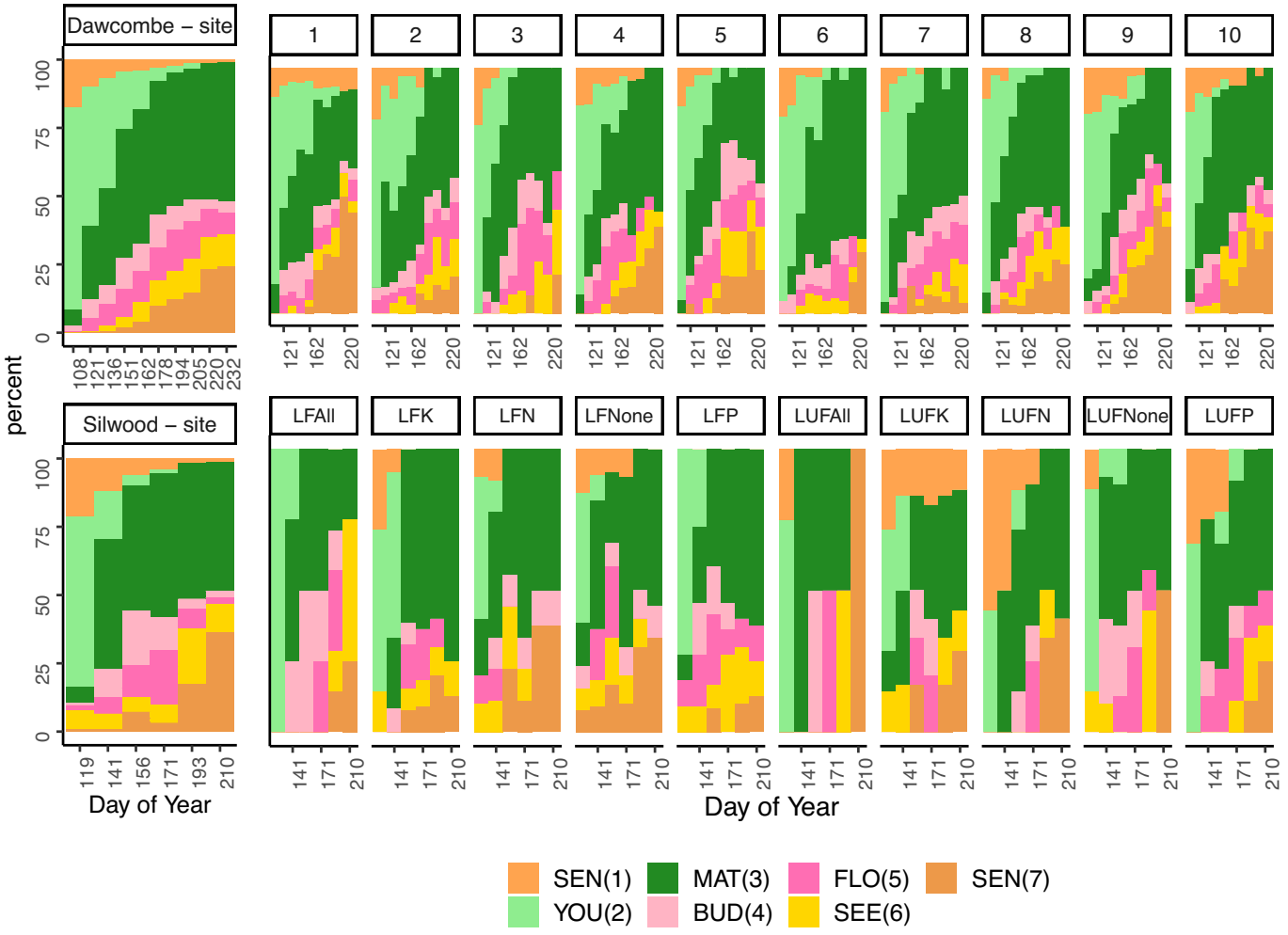

Fig. 5. The percentage of the canopy dominated by each of the seven documented phenological stages at each time point over the growing season at the site and the quadrat level.

Dawcombe, young material was still emerging in all quadrats up to DoY 194 and 205, towards the end of the phenology period NDVI-max. YOU (2) material was absent in all quadrats during the last two sampling points (DoY 220 and 232). Peak MAT(3) was reached on DoY 151 at Dawcombe and occurred at the cusp of the two satellite derived phenology stages (pre-NDVI-max and NDVI-max). At Silwood, peak MAT(3) was recorded at DoY 171, well into the NDVI-max satellite period. The percentage of the sward in stages BUD(4), FLO(5) or SEE(6) (bud, flowering or seed respectively) was very variable between quadrats at any one time.

3.2. Spectral CoV over time

Mean reflectance values per quadrat, per sampling time are shown in Fig. 6a and 6b alongside changes in the spectral variance for each wavelength. Mean reflectance for some quadrats (quadrat 5 at Dawcombe and quadrat LUFP at Silwood for example) remained very stable throughout the season whereas other quadrats displayed clear seasonal shifts (quadrat 4 at Dawcombe and quadrat LUFAll at Silwood). The largest magnitude in changes is observed in the NIR part of the spectrum. Seasonal patterns in CoV also changed dramatically in some quadrats but not in others. The temporal change in spectral variability were evaluated by the slope of a linear regression model CoV = f(DoY) for each quadrat (See Supplementary Material B, Table B1). Within quadrat rates of change were not very different between the spectral regions and the extent of change was principally a cross spectra phenomenon, therefore, only the mean-CoV is reported here. At Dawcombe quadrats 2, 3, 5 and 8 remained stable in time (model slope close to zero) whereas quadrats 1, 4, 6, 7, 9, and 10 increased over time (model slopes $> +0.1$, the fastest changing quadrat was quadrat 6 at $+0.34$). At Silwood, quadrats LFK and LUFK were stable, whereas all other quadrats at this site increased in spectral variability as the season progressed (with the maximum rate of change found at quadrat LFNone, model slope $+$ 0.47).

At the site level, mean-CoV followed the same overall trajectory at both sites, starting at a low level and increasing as the season progressed

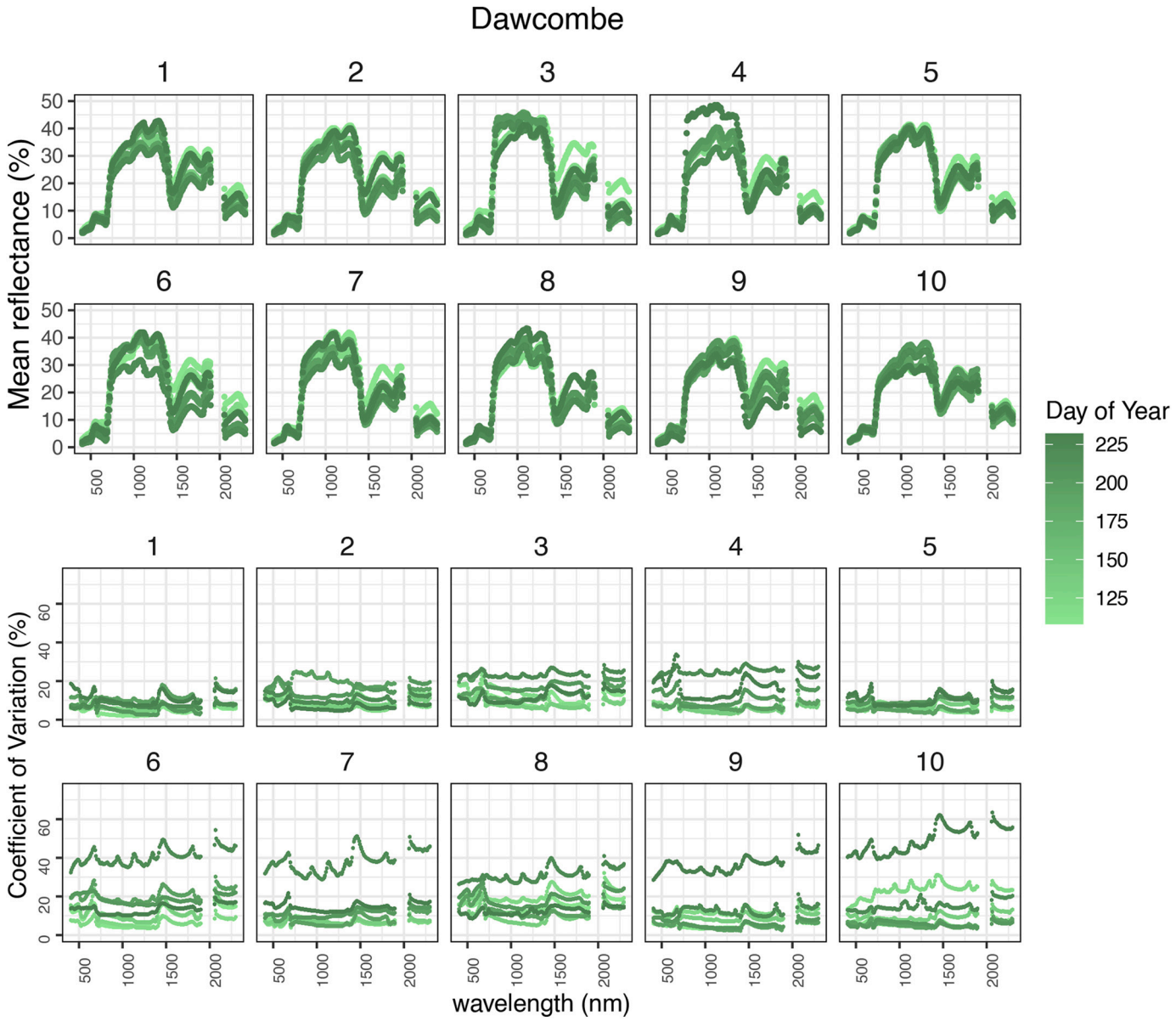

Fig. 6. a: Mean spectral reflectance and Coefficient of Variation (CoV) per quadrat per wavelength over the sampling days from the quadrat-based spectrometry data for Dawcombe. b: Mean spectral reflectance and Coefficient of Variation (CoV) per quadrat per wavelength over the sampling days from the quadrat-based spectrometry data for Silwood.

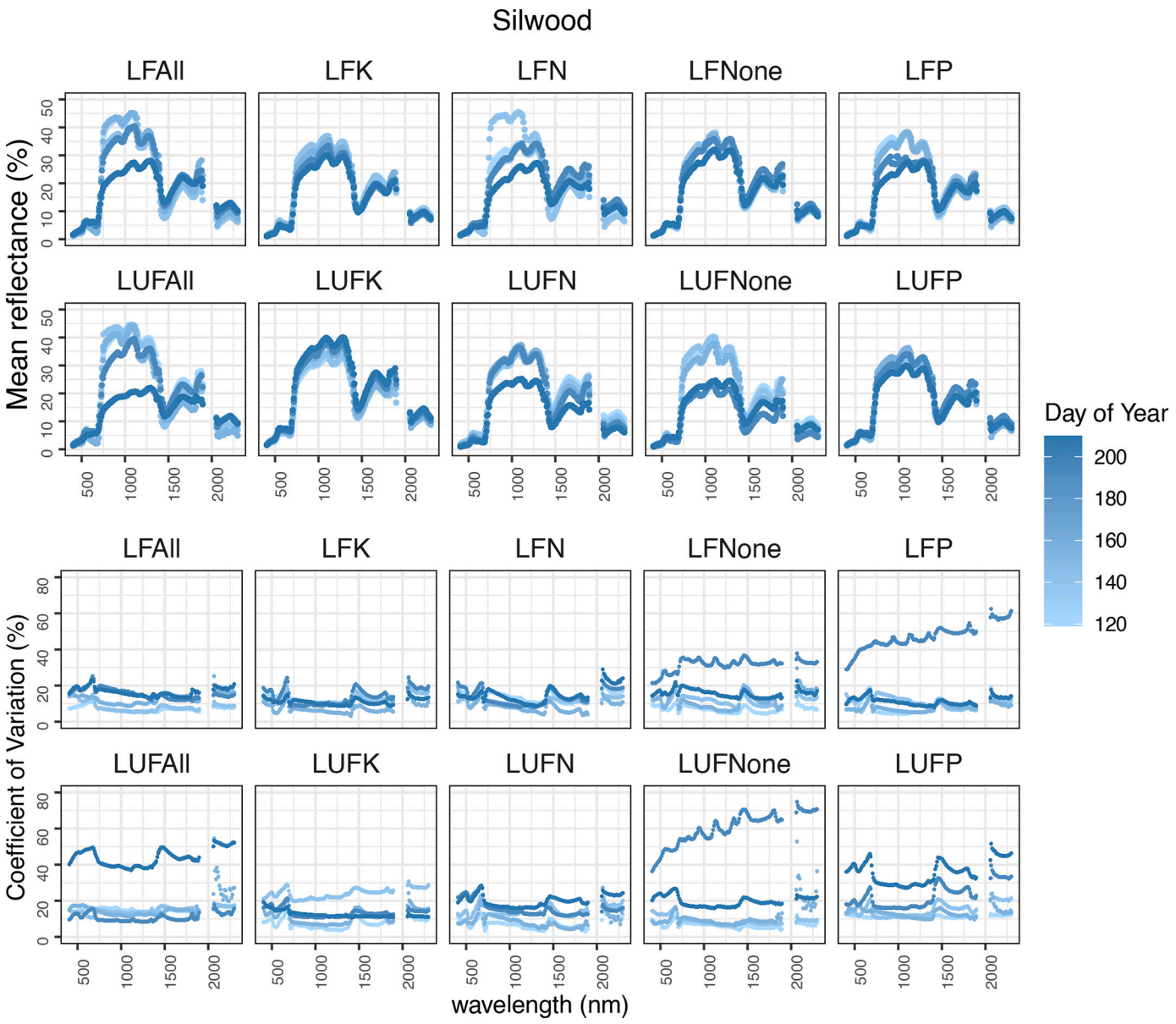

Fig. 6. (*continued*).

through pre-NDVI max and NDVI max, with the highest values occurring in late summer during post-NDVI max (Figs. 6 and 7). The extent to which the CoV changed over time is expressed as the slope of a linear regression model (Dawcombe $r^2 = 0.18$, $p = 0.00021$ (2sf), slope = +0.08 and Silwood $r^2 = 0.20$, $p = 0.000069$, slope = +0.15). The rate of change was slightly higher at Silwood in all spectral regions compared to Dawcombe.

3.3. The relationship between spectral diversity (CoV) and taxonomic and phenological diversity using linear permutation models

3.3.1. The spectral regions approach

The strength of the relationship between spectral variance averaged across spectral regions and each of the six uni-temporal plant community metrics (species richness, species evenness, species diversity, phenological richness, phenological evenness and phenological diversity) was very variable across time (Fig. 8), indicating that at the quadrat level spectral variance does not track changes in these metrics over a season. Values of adjusted r^2 for 209 out of 288 of the models were less than 0.1, meaning that at the majority of sampling points and for most community variables very little variation, if any, was explained by the metrics. Twenty-five out of 288 of the models were significant at $p < 0.05$. In eight of these models, mean-CoV was the predictor variable, in four, vis-mean-CoV, in seven, NIR-mean-CoV and in six, SWIR-mean-CoV. Three of the significant models predicted well values of phenological diversity, six phenological evenness, five phenological richness, six species diversity, one species evenness and four species richness (see Table 4). The sampling times when spectral variance best predicted taxonomic diversity (highest r^2 values and significant models) was at the end of pre-NDVI max (DoY 136) and post-NDVI-max (DoY 220 and 232) for Dawcombe and during NDVI-max (DoY 156) for Silwood.

The stability of the model r^2 also depended on the level of data cleaning imposed by the alpha parameter in the ROBPCA (Supplementary Material, Section A Fig. A1 and A2). At some time points, model r^2 steadily increased with more robust data cleaning. For example, at Dawcombe, Phenological diversity at DoY 194, during NDVI-max and Phenological evenness and diversity at DoY 136, during pre-NDVI-max, displayed this behaviour. Other model r^2 values remained constant, despite the level of data cleaning, for example for species evenness and species diversity at DoY 108. These results suggests that, at times, the

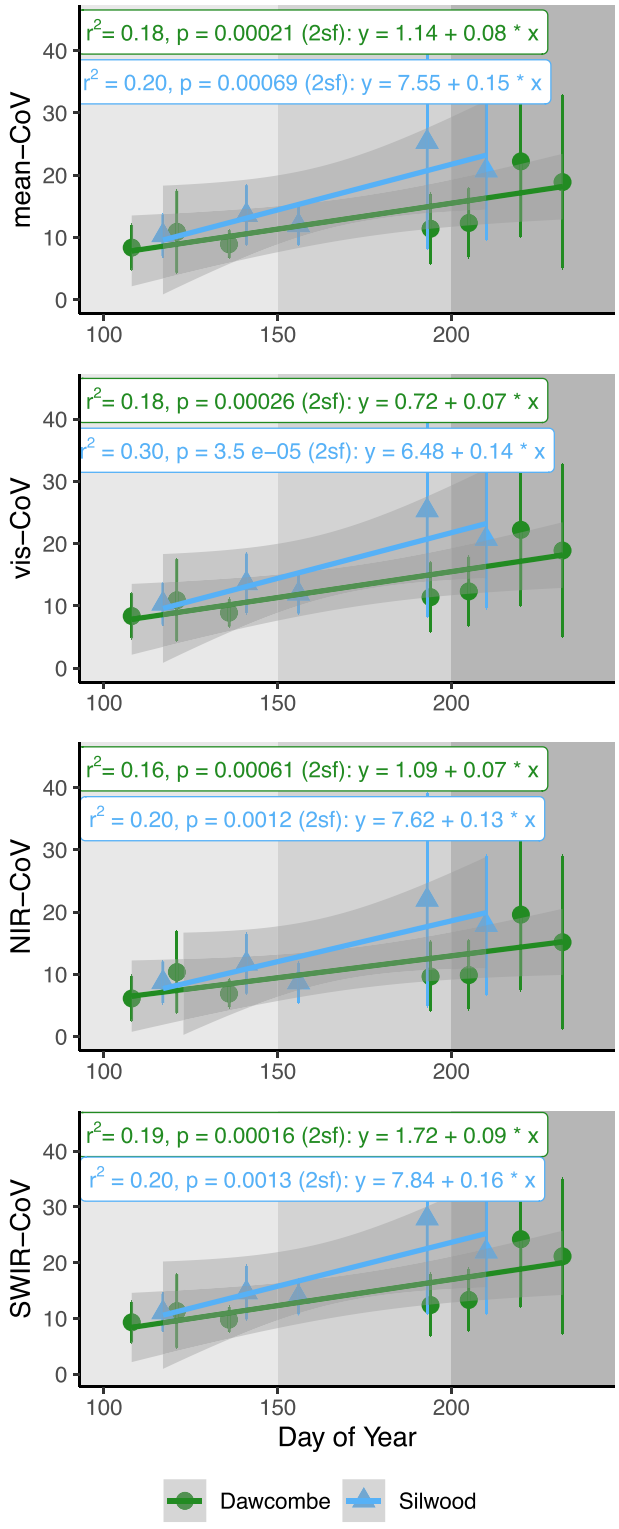

Fig. 7. Mean-CoV and spectral-regions-CoV over time, with linear model results describing the temporal increase at the site level.

quadrat level CoV can depend on a few reflectance outliers caused by, for example, bare soil, or a single plant dominating a sub quadrat or measurement errors such as un-intended off-nadir viewing. Our confidence in the SVH should increase with models that remain stable or improve in fit with data cleaning.

3.3.2. The hyperspectral approach

The linear permutation models were also applied to spectral variance at the hyperspectral level. The adjusted r^2 of these models is reported in Fig. 9. At Dawcombe at DoY 220 and 232, the whole of the spectrum displayed strong correlations to the metrics, however, at DoY 136 only narrow regions of the spectrum were correlated. Examination of the model fits from the hyperspectral approach demonstrated that the spectral regions approach was largely effective at picking up the best sampling times and metrics of interest.

3.4. Mixed models: relationships between variables over time

All the spectral data, summarised as spectral regions (the spectral regions approach), was included in a series of mixed models, allowing for temporal and spatial pseudo-replication. In the first stage of mixed modelling, which tested the ability of the CoV of spectral variance to predict taxonomic or phenological metrics over all sampling times and both sites, none of the models contained significant terms (see Supplementary Material C, Table C1). A large amount of variance in these models was explained by the random terms. Values of the Intra-class Correlation Coefficient (ICC) (the ratio of the between group variance to the total variance) (Nakagawa et al., 2017) ranged from 0.32–0.43 (these are considered high values and validify the use of the mixed model approach). The random term, quadrat, had a much smaller impact on the model, with estimates of around 10% that of sampling-time. These results further support the results from the uni-temporal models, that the strength of the relationship between spectral variance and these metrics is heavily time dependent.

During the second stage of mixed modelling, differing interaction effects of percent phenology stage dominance (SEN(1), YOU(2), MAT (3), BUD(4), FLO(5), SEE(6), SEN(7)) and taxon and phenology-based community metrics on spectral variance were tested. A significant effect of MAT(3) mature stage (slope = 0.19, $p = 0.003$) alongside a significant interaction effect of MAT(3) and species diversity (slope = 0.12, $p = 0.014$) was found for mean-CoV (Fig. 10) with similar results for the other spectral regions (see Supplementary Material C, Table C2 for full model results). NIR was the spectral region with the highest marginal r^2, with around 25% of the variance explained by the fixed terms, and an effect size of 0.25 for the mature term and 0.15 for the interaction term mature and species diversity. The model using vis-mean-CoV as the response variable displayed the largest values of conditional r^2 with 43% variance explained, 16% of which was explained by the fixed terms.

4. Discussion

4.1. Relationships between spectral variance and taxonomic and phenology metrics over time

The uni-temporal models at the site level were able to predict gradients of both taxonomic and phenology-based community metrics. However, the predictive ability of the models varied over time indicating that tracking these metrics across a growing season using spectral variation is problematic. The highest correlations between spectral and community metrics tended towards late pre-NDVI-max and early NDVI-max at both sites, suggesting that late spring (around DoY 150) is optimal for estimation of taxonomic and phenological traits in these grassland systems. These dates coincided with maximum species and phenological diversity at both sites. Late summer sampling (DoY 220 and 232 during post-NDVI-max) also proved productive at Dawcombe, although data was not collected on comparable dates for Silwood due to the site management regime. Using the mixed model approach, we found that none of the six metrics displayed a consistent relationship to spectral variance over time, further confirming that there is a temporal dependence in the relationship.

However, at the low species diversity site, Silwood, the best models (DoY 156) consistently predicted a negative relationship between the

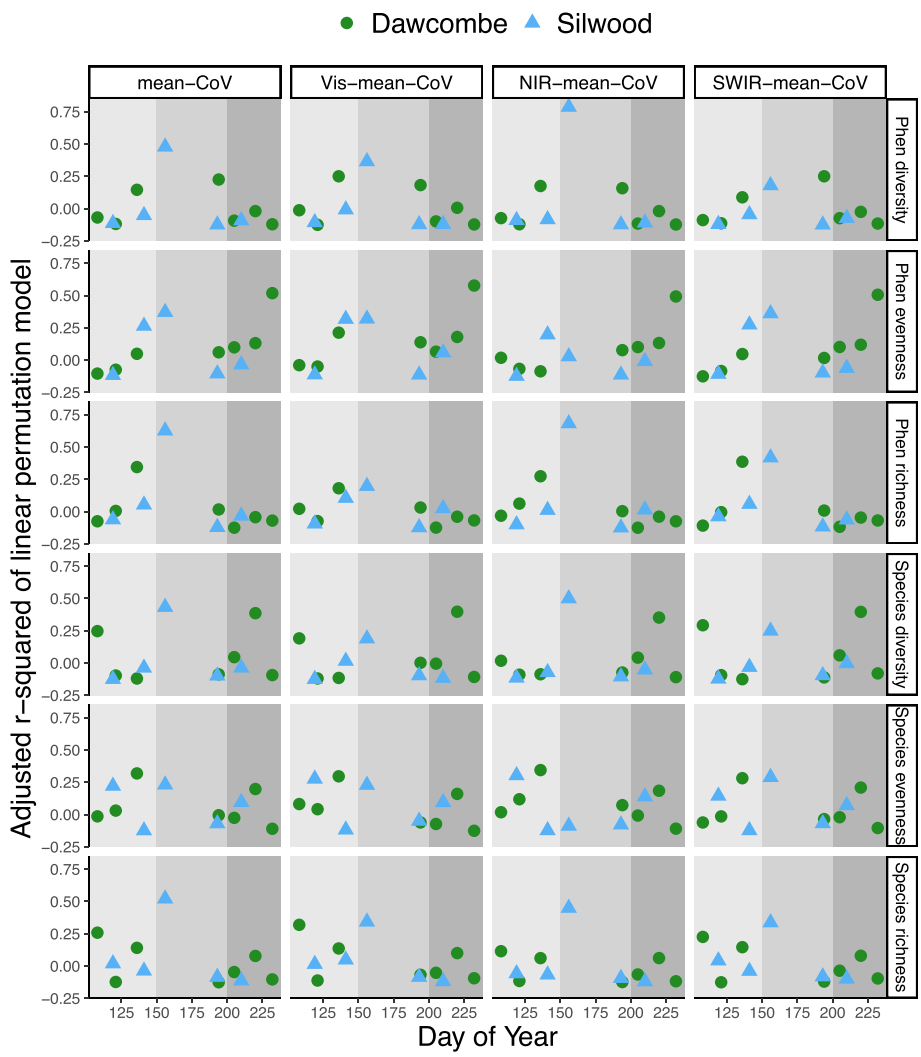

Fig. 8. Adjusted r^2 of the simple uni-temporal linear permutation models (spectral variance = f(diversity metric) using the spectral regions approach.

metrics and spectral variance, for five out of six of the metrics (none of the models predicted well Species Evenness). At Dawcombe, regardless of the sampling time, for the best models, there was always a positive relationship between spectral variance and the metrics; a result that supports the SVH (note that species and phenological evenness should under the hypothesis display a negative relationship, as low measures of evenness represent more varied communities).

We proposed that grassland community phenological dynamics could be responsible for some of the variation in spectral variance. We tested this hypothesis using our own phenological metrics and looked for interactions between these metrics and the species-based metrics in a mixed modelling approach. However, we found no significant interaction terms, implying that phenology-based spectral signals are not operating systematically across the growing season either to detract from species-based signals or to enhance them.

When considering the overall trend in spectral variance between sites, despite Silwood and Dawcombe displaying low and high taxonomic and phenological diversity, respectively, the mean-CoV values at the site level were marginally higher at Silwood (Fig. 7) clearly demonstrating that, in this instance, the site with the higher diversity did not have a higher spectral variance.

4.2. Taxonomic and phenological dynamics between sites

The trends in taxonomic and phenology metrics show how grasslands can display diverse temporal dynamics in terms of the seasonal development of their community composition which may have effects on our ability to monitor them using remote sensing techniques and the SVH. Judging from these results if we want to capture the full extent of taxonomic and phenological diversity we should sample just before and during NDVI-max. We speculate that both spring and summer emerging species are occurring simultaneously at this time, thus maximising measures of both species and phenological diversity. We observed that at Silwood the phenology and taxonomic metrics were more strongly correlated across the season than at Dawcombe (Fig. 4). This suggests that at Silwood phenological diversity follows seasonal species turnover whereas at Dawcombe there is a more complex relationship. This complexity could be a direct result of the higher species diversity of the site or the type of species present. It could also reflect other phenomena such as assortative mating and the development of discrete sub-populations that over time become reproductively isolated (Elzinga et al., 2007).

4.3. Mature leaves as drivers of spectral variance

Across the growing season, at the site level an increase in spectral variance was observed, which was found to be independent of the taxonomic and phenological based metrics. Rather spectral variance was found to be partly driven by the occurrence of plant parts in MAT(3) phenology stage. There are different possible interpretations of this

Table 4
Results of the significant uni-temporal permutation models at $p < 0.05$. Results that do **not** support the SVH are highlighted in **grey**.

Site	Time Point	DoY	Satellite derived phenology stage	Community metric	Spectral variable	(Coefficient) Intercept	(Coefficient) Slope	adjusted r^2	p value
Dawcombe	**3**	136	Pre-NDVI-max	Species evenness	NIR-mean-CoV	8.652	**-13.775**	**0.345**	**0.043**
Dawcombe	**9**	220	Post-NDVI-max	Species diversity	mean-CoV	31.025	**7.716**	**0.387**	**0.032**
Dawcombe	**9**	220	Post-NDVI-max	Species diversity	NIR-mean-CoV	28.028	**6.770**	**0.353**	**0.041**
Dawcombe	**9**	220	Post-NDVI-max	Species diversity	SWIR-mean-CoV	33.774	**8.797**	**0.397**	**0.030**
Dawcombe	**9**	220	Post-NDVI-max	Species diversity	vis-mean-CoV	27.855	**6.006**	**0.398**	**0.030**
Dawcombe	**3**	136	Pre-NDVI-max	Phenological richness	mean-CoV	11.055	**2.129**	**0.345**	**0.043**
Dawcombe	**3**	136	Pre-NDVI-max	Phenological richness	SWIR-mean-CoV	12.307	**2.676**	**0.387**	**0.032**
Dawcombe	**10**	232	Post-NDVI-max	Phenological evenness	mean-CoV	27.107	**-129.600**	**0.519**	**0.011**
Dawcombe	**10**	232	Post-NDVI-max	Phenological evenness	NIR-mean-CoV	23.407	**-115.058**	**0.493**	**0.014**
Dawcombe	**10**	232	Post-NDVI-max	Phenological evenness	SWIR-mean-CoV	29.626	**-144.397**	**0.507**	**0.013**
Dawcombe	**10**	232	Post-NDVI-max	Phenological evenness	vis-mean-CoV	26.114	**-109.356**	**0.578**	**0.006**
Silwood	**3**	156	NDVI-max	Species richness	mean-CoV	13.237	**-0.803**	**0.521**	**0.011**
Silwood	**3**	156	NDVI-max	Species richness	NIR-mean-CoV	9.453	**-0.712**	**0.449**	**0.020**
Silwood	**3**	156	NDVI-max	Species richness	SWIR-mean-CoV	15.341	**-0.892**	**0.337**	**0.046**
Silwood	**3**	156	NDVI-max	Species richness	vis-mean-CoV	13.791	**-0.688**	**0.342**	**0.044**
Silwood	**3**	156	NDVI-max	Species diversity	mean-CoV	13.237	**-1.029**	**0.433**	**0.023**
Silwood	**3**	156	NDVI-max	Species diversity	NIR-mean-CoV	9.453	**-1.024**	**0.499**	**0.013**
Silwood	**3**	156	NDVI-max	Phenological richness	mean-CoV	13.237	**-1.528**	**0.626**	**0.004**
Silwood	**3**	156	NDVI-max	Phenological richness	NIR-mean-CoV	9.453	**-1.490**	**0.682**	**0.002**
Silwood	**3**	156	NDVI-max	Phenological richness	SWIR-mean-CoV	15.341	**-1.707**	**0.418**	**0.026**
Silwood	**3**	156	NDVI-max	Phenological evenness	mean-CoV	13.237	**9.911**	**0.371**	**0.036**
Silwood	**3**	156	NDVI-max	Phenological evenness	SWIR-means-CoV	15.341	**12.890**	**0.360**	**0.039**
Silwood	**3**	156	NDVI-max	Phenological diversity	mean-CoV	13.237	**-0.051**	**0.478**	**0.016**
Silwood	**3**	156	NDVI-max	Phenological diversity	NIR-mean-CoV	9.453	**-0.059**	**0.787**	**0.000**
Silwood	**3**	156	NDVI-max	Phenological diversity	vis-mean-CoV	13.791	**-0.046**	**0.365**	**0.038**

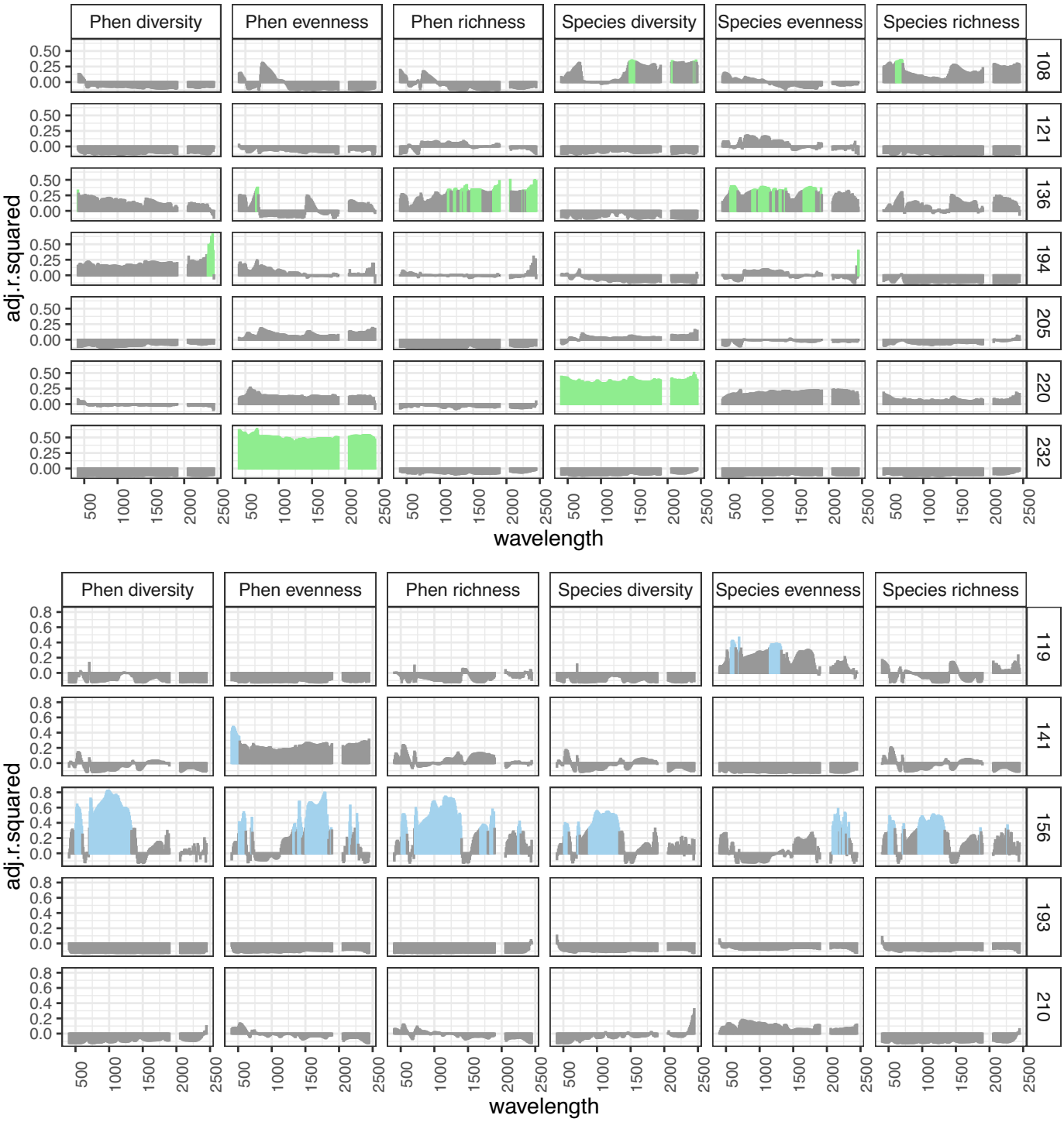

Fig. 9. Adjusted r^2 of the simple uni-temporal linear permutation models (spectral variance = f(metric) using the hyperspectral approach. Significant wavelengths are shown in colour; non-significant in grey.

result. Firstly, mature leaves of plants could, in fact, be more spectrally variable than other leaf growth stages. Another perspective is that when plants are in their mature stages canopy structural attributes contribute to spectral variance through self-shading. This problem is difficult to eliminate in mixed 'pixel' situations, but if the pixel sizes were small enough (i.e., those obtained through drone acquisition), this problem could be reduced through removal of low NDVI 'shade' pixels, in a similar way to soil correction techniques (Gholizadeh et al., 2018). Additionally, as canopies develop over time, they could become more spectrally variable due to vertical complexity (Conti et al., 2021). The mixed model with the highest explained variance by the fixed terms (MAT(3) and species diversity) was in the NIR spectral region. This suggests that canopy traits such as LAI and leaf angle distribution could be influential.

Irrespective of the ultimate driver of spectral variance associated with the presence of mature leaves, the observed underlying seasonal increase in spectral variance needs to be taken into account when sampling across dates for the purposes of taxonomic diversity evaluation as it will likely confound the desired signal. The observed interaction effect of species diversity and mature leaves implies that the usefulness

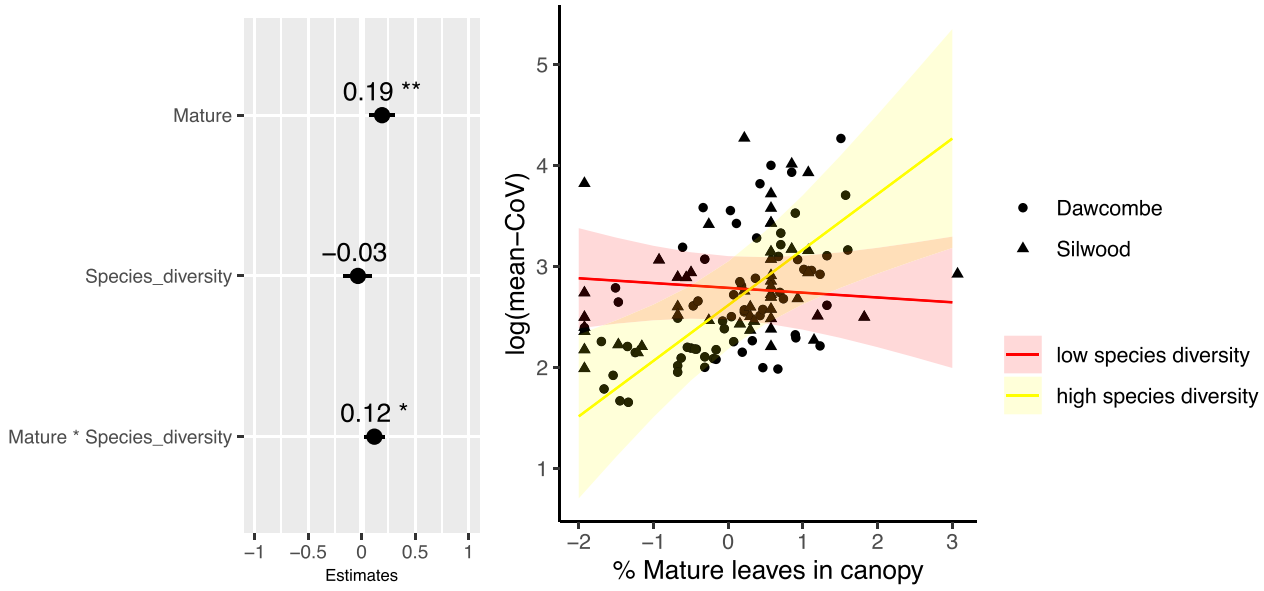

Fig. 10. Left: Forest plot showing the standardised effect sizes of the fixed terms in the mixed model; percent mature leaves (MAT(3)) species diversity and their interaction term.
Right: Significant interaction effect of MAT(3) and species diversity on mean spectral variance. Prediction lines with confidence intervals show values of species diversity at extremes of the data set ($D_t = 1$ and 13). MAT(3) is scaled with values ranging from $-2 = 0\%$ and $+3 = 100\%$).

of spectral variance as a surrogate for species diversity is dependent on the extent to which plant species are synchronous in terms of their display of mature leaves.

4.4. Issues of scale in estimations of species diversity

One of the major challenges in testing the SVH is that the strength of findings may rely on both the temporal *and* spatial scale of the observations. Here we investigated whether the species diversity of small grassland plots could be predicted using very high resolution (10 cm^2) simulated pixels. A similar study in grasslands showed significant correlations between spectral variance and species diversity at single points in time (Wang et al., 2018) and demonstrated that spectral variance calculated using the smallest pixels (1mm^2) had the strongest relationship to taxonomic-based metrics, with the relationship declining as pixel size increased and 10 cm^2 pixels being the largest size at which the relationship held. A possible explanation for this decline in the relationship with increased scale is that species diversity metrics per quadrat may not be well aligned to the spectral data. Consider the situation where one quadrat has many species but they are small and evenly distributed throughout the quadrat. This situation is typical of the quadrats at Dawcombe in the species rich calcareous grassland. The spectral diversity of this quadrat at 10 × 10 cm pixel resolution could be very low, as each of the pixels are very similar. Compare this to a quadrat with only two species that are distributed in clumps and spectrally dissimilar. In contrast the spectral diversity of this quadrat could be high. To adequately assess community complexity using reflectance data our plant diversity metrics need to be robust in light of this type of dilemma with consideration given to the appropriate pixel size scaling to the community at hand.

We tested the SVH using both the spectral regions approach and the hyperspectral approach. In this instance, the models fitted using the spectral variance of very narrow wavelengths did not perform better, or provide more insight, than using broad spectral bands (regions) in terms of the timing of sampling nor the taxonomic or phenological metrics. Wang et al., 2018 also showed that summary measures of variance taken across the spectrum were sufficient to predict species diversity. However, other previous studies have demonstrated that species discrimination is possible only by small differences in reflectance in narrow bands (Kokaly et al., 2003; Schmidt and Skidmore, 2003). These results suggest that high spectral resolution data may be less important for diversity studies than for detecting species classes.

4.5. Challenges and further study: other sources of spectral variance in grasslands

Diversity in temperate grasslands has been shown to be a product of structural lack of species dominance in the canopy and light 'sharing' (Borer et al., 2014; Pulungan et al., 2019). Diverse grasslands by consequence have sparser canopies, are lower in absolute biomass and are usually found in soils lower in nutrients (which determines the absence of nitrophiles, that tend to dominate the canopy) (Crawley et al., 2005; Silvertown et al., 2006). Grasslands that follow this definition may be detectable by virtue of their canopy structural parameters such as height and LAI (Stenzel et al., 2017). It is possible that the negative relationship between spectral variance and the diversity metrics at Silwood is linked to these variables. Self-shading or vertical complexity as a source of spectral variation in high biomass swards could be additional sources of variation at this small scale. At this site, high spectral variance was found in high fertilizer addition plots with single species (LUFAll at DoY 210) alongside a large seasonal growth in CoV (model slope 0.23–0.29 depending on spectral region, see supplementary material table B1). In this instance, we could say that high levels of intra-specific spectral variation are displayed as this change is not associated with changes in species composition.

The principal challenge in interpreting the results of this study is that we don't know the relative importance of leaf and canopy traits in driving spectral variance over time. A future option would be to monitor biomass variation both between sampling points and within a sampling unit. It is obviously impossible to monitor changes in biomass within a quadrat using destructive sampling techniques. However, biomass models using non-destructive measures of LAI and NDVI, in partnership with radiative transfer modelling, have been shown to provide reasonably accurate time-series of fluctuations (Punalekar et al., 2018). Some traits could therefore be simulated from spectral data. Future studies into the relationship between spectral variance and diversity metrics should attempt to incorporate at least some other leaf and canopy traits.

Temporal variability in the relationship between floristic patterns

and spectral response in grasslands have been demonstrated in other studies using multi-temporal hyperspectral sampling and the physical model, PROSAIL (Feilhauer et al., 2017). In this case, the driver of spectral variability was found to be local resource stressors (i.e., leaf dehydration) and had little to do with changes in the actual canopy composition. In other multi-temporal studies, seasonal burning of the sward was proposed to be responsible for the failure of spectral variance to predict species diversity in some years (Gholizadeh et al., 2020). Large scale disturbance events could be associated with a re-setting of phenological niche partitioning that drives phenological diversity causing the relationship between spectral variance and plant community diversity to break down.

The observation that the amount of data cleaning changed the strength of the relationship between spectral variance and the taxonomic and phenology metrics also deserves further investigation. We may expect that in the early part of the growing season bare soil may be present in certain sub-quadrats. By recording total vegetation cover per plot it would be possible to infer if reflectance measurements were being affected by the present of bare ground. Later in the season, some plants with erect growth forms could cast shadow on other plants that display a more recumbent habit. Alongside erroneous data, these are the kinds of spectra that require filtering from the dataset. Ensuring the correct level of data cleaning and the most appropriate methods remain significant challenges.

5. Conclusion

Results of this study suggest that spatial variability in reflectance fails to hold across space and time as a predictor of species diversity in grasslands. It appears that at a single point in time stochastic combinations of species and/or phenological traits of canopies can drive spectral diversity. This may explain the instability of previous studies that examine similar questions. We observe that for these grasslands the canopy stage MAT(3) is positively correlated with canopy spectral variance over the season and that if this canopy stage is accounted for there may be an opportunity to predict well species diversity using these data. The full reasons for these observations remain unclear and we highlight the need for simultaneous collection of some leaf and canopy traits in future similar studies to help determine the cause.

The fact that species and phenological properties of canopies were comparably estimated in the uni-temporal models suggests that spectral variance may be *at least as* suitable for looking at phenological properties as taxonomic ones. Establishing a link between spectral variance and phenological patterning of grassland communities would be an important addition to the study of plant phenology and conservation biology (Morellato et al., 2016) as well as furthering our understanding of the effects of climate change on species phenological partitioning.

Under current knowledge, application of the SVH to within-site monitoring of taxonomic diversity should be approached with caution. More studies are required that incorporate multiple sampling dates, at differing spatial scales, to determine if the relationship is stable enough to be useful in ecological evaluations. However, verifying the results of this study by expanding the geographical extent of detailed multi-temporal studies will remain a significant challenge due to the time-consuming nature of repeat botanical and spectral sampling at a gradient of spatial resolutions.

Authorship contribution statement

Rachael Thornley: conceptualisation, spectral and botanical data collection, data analysis and writing. France Gerard: conceptualisation, review and editing. Kevin White: conceptualisation, data collection, technical guidance on instruments, review and editing. Anne Verhoef: conceptualisation, data collection, review and editing.

Declaration of Competing Interest

The authors declare that they have no known competing financial interests or personal relationships that could have appeared to influence the work reported in this paper.

Acknowledgements

RT was supported by a NERC (Natural Environment Research Council) studentship grant NE/L002566/1. Use of the SVC spectrometers in dual mode was enabled by an equipment loan through the NERC Field Spectroscopy Facility. We wish to thank Surrey Wildlife Trust and Simon Humphreys for access to Dawcombe nature reserve and Imperial College London for access to Nash's Field Long Term Experiment at Silwood Park. The authors are also grateful to Petra Guy, Rob Fry, Catalina Estrada and Charles George for help with setting up quadrats and data collection. Statistical advice on mixed models was given by Peter Henrys at the UK Centre for Ecology and Hydrology, Lancaster. In addition, we wish to thank two anonymous reviewers for their considerable contribution in improving the message and clarity of this research presentation.

Appendix A. Supplementary data

Supplementary data to this article can be found online at https://doi.org/10.1016/j.rse.2022.112908.

References

Ali, I., Cawkwell, F., Dwyer, E., Barrett, B., Green, S., 2016. Satellite remote sensing of grasslands: from observation to management. J. Plant Ecol. 9 (6), 649–671.

Aragón, R., Oesterheld, M., Irisarri, G., Texeira, M., 2011. Stability of ecosystem functioning and diversity of grasslands at the landscape scale. Landsc. Ecol. 26 (7), 1011–1022 [Online]. https://doi.org/10.1007/s10980-011-9625-z.

Asner, G.P., 1998. Biophysical and biochemical sources of variability in canopy reflectance. Remote Sens. Environ. 64 (3), 234–253. https://doi.org/10.1016/S0034-4257(98)00014-5.

Asner, G.P., Martin, R.E., 2011. Canopy phylogenetic, chemical and spectral assembly in a lowland Amazonian forest. New Phytol. 189 (4), 999–1012. https://doi.org/10.1111/j.1469-8137.2010.03549.x.

Asner, G.P., Martin, R.E., 2016. Spectranomics: emerging science and conservation opportunities at the interface of biodiversity and remote sensing. Glob. Ecol. Conserv. 8, 212–219.

Asner, G.P., Martin, R.E., Ford, A.J., Metcalfe, D.J., Liddell, M.J., Asner, G.P., Martin, R. E., Ford, A.J., Metcalfe, D.J., Liddell, M.J., 2009. Leaf chemical and spectral diversity in Australian Tropical forests, 19 (1), 236–253.

Barr, D.J., Levy, R., Scheepers, C., Tily, H.J., 2013. Random effects structure for confirmatory hypothesis testing: keep it maximal. J. Mem. Lang. 68 (3), 255–278. https://doi.org/10.1016/j.jml.2012.11.001.

Bates, D., Mächler, M., Bolker, B., Walker, S., 2015. Fitting linear mixed-effects models using lme4. J. Stat. Softw. 67 (1), 1–48.

Blanco-Sacristán, J., Panigada, C., Tagliabue, G., Gentili, R., Colombo, R., de Guevara, M. L., Maestre, F.T., Rossini, M., 2019. Spectral diversity successfully estimates the α-diversity of biocrust-forming lichens. Remote Sens. 11 (24), 1–16 [Online]. https://doi.org/10.3390/rs11242942.

Borer, E.T., Seabloom, E.W., Gruner, D.S., Harpole, W.S., Hillebrand, H., Lind, E.M., Adler, P.B., Alberti, J., Anderson, T.M., Bakker, J.D., Biederman, L., Blumenthal, D., Brown, C.S., Brudvig, L.A., Buckley, Y.M., Cadotte, M., Chu, C., Cleland, E.E., Crawley, M.J., Daleo, P., Damschen, E.I., Davies, K.F., Decrappeo, N.M., Du, G., Firn, J., Hautier, Y., Heckman, R.W., Hector, A., Hillerislambers, J., Iribarne, O., Klein, J.A., Knops, J.M.H., La Pierre, K.J., Leakey, A.D.B., Li, W., MacDougall, A.S., McCulley, R.L., Melbourne, B.A., Mitchell, C.E., Moore, J.L., Mortensen, B., O'Halloran, L.R., Orrock, J.L., Pascual, J., Prober, S.M., Pyke, D.A., Risch, A.C., Schuetz, M., Smith, M.D., Stevens, C.J., Sullivan, L.L., Williams, R.J., Wragg, P.D., Wright, J.P., Yang, L.H., 2014. Herbivores and nutrients control grassland plant diversity via light limitation. Nature 508 (7497), 517–520 [Online]. https://doi.org/10.1038/nature13144.

Chavana-Bryant, C., Malhi, Y., Wu, J., Asner, G.P., Anastasiou, A., Enquist, B.J., Cosio Caravasi, E.G., Doughty, C.E., Saleska, S.R., Martin, R.E., Gerard, F.F., 2017. Leaf aging of Amazonian canopy trees as revealed by spectral and physiochemical measurements. New Phytol. 214 (3), 1049–1063 [Online]. https://doi.org/10.1111/nph.13853.

Conti, L., Malavasi, M., Galland, T., Komárek, J., Lagner, O., Carmona, C.P., de Bello, F., Rocchini, D., Šímová, P., 2021. The relationship between species and spectral diversity in grassland communities is mediated by their vertical complexity. Appl. Veg. Sci. 24 (3), 1–8 [Online]. https://doi.org/10.1111/avsc.12600.

Crawley, M.J., Johnston, A.E., Silvertown, J., Dodd, M., de Mazancourt, C., Heard, M.S., Henman, D.F., Edwards, G.R., 2005. Determinants of species richness in the park grass experiment. Am. Nat. 165 (2), 179–192. https://doi.org/10.1086/427270.

Denny, E.G., Gerst, K.L., Miller-Rushing, A.J., Tierney, G.L., Crimmins, T.M., Enquist, C. A.F., Guertin, P., Rosemartin, A.H., Schwartz, M.D., Thomas, K.A., Weltzin, J.F., 2014. Standardized phenology monitoring methods to track plant and animal activity for science and resource management applications. Int. J. Biometeorol. 58 (4), 591–601 [Online]. https://doi.org/10.1007/s00484-014-0789-5.

Elzinga, J.A., Atlan, A., Biere, A., Gigord, L., Weis, A.E., Bernasconi, G., 2007. Time after time: flowering phenology and biotic interactions. Trends Ecol. Evol. 22 (8), 432–439 [Online]. https://doi.org/10.1016/j.tree.2007.05.006.

Fassnacht, F.E., Latifi, H., Stereńczak, K., Modzelewska, A., Lefsky, M., Waser, L.T., Straub, C., Ghosh, A., 2016. Review of studies on tree species classification from remotely sensed data. Remote Sens. Environ. 186, 64–87 [Online]. https://doi.org/10.1016/j.rse.2016.08.013.

Fava, F., Parolo, G., Colombo, R., Gusmeroli, F., Della Marianna, G., Monteiro, A.T., Bocchi, S., 2010. Fine-scale assessment of hay meadow productivity and plant diversity in the European Alps using field spectrometric data. Agric. Ecosyst. Environ. 137 (1–2), 151–157. Elsevier B.V. [Online]. https://doi.org/10.1016/j.agee.2010.01.016.

Feilhauer, H., Schmidtlein, S., 2011. On variable relations between vegetation patterns and canopy reflectance. Ecol. Inform. 6 (2), 83–92. Elsevier B.V. [Online]. https://doi.org/10.1016/j.ecoinf.2010.12.004.

Feilhauer, H., Somers, B., van der Linden, S., 2017. Optical trait indicators for remote sensing of plant species composition: predictive power and seasonal variability. Ecol. Indic. 73, 825–833. Elsevier Ltd. [Online]. https://doi.org/10.1016/j.ecolind.2016.11.003.

Forrest, J., Miller-Rushing, A.J., 2010. Toward a synthetic understanding of the role of phenology in ecology and evolution. Philos. Trans. Royal Soc. B: Biol. Sci. 365 (1555), 3101–3112 [Online]. https://doi.org/10.1098/rstb.2010.0145.

Gamon, J.A., Somers, B., Malenovský, Z., Middleton, E.M., Rascher, U., Schaepman, M. E., 2019. Assessing vegetation function with imaging spectroscopy. Surv. Geophys. 40 (3), 489–513. Springer Netherlands. [Online]. https://doi.org/10.1007/s10712-019-09511-5.

Gholizadeh, H., Gamon, J.A., Zygielbaum, A.I., Wang, R., Schweiger, A.K., Cavender-Bares, J., 2018. Remote sensing of biodiversity: soil correction and data dimension reduction methods improve assessment of α-diversity (species richness) in prairie ecosystems. Remote Sens. Environ. 206 (December 2017), 240–253. Elsevier. [Online]. https://doi.org/10.1016/j.rse.2017.12.014.

Gholizadeh, H., Gamon, J.A., Helzer, C.J., Cavender-Bares, J., 2020. Multi-temporal assessment of grassland α- and β-diversity using hyperspectral imaging. Ecol. Appl. 0 (0), 1–13 [Online]. https://doi.org/10.1002/eap.2145.

Hall, K., Johansson, L.J., Sykes, M.T., Reitalu, T., Larsson, K., Prentice, H.C., 2010. Inventorying management status and plant species richness in seminatural grasslands using high spatial resolution imagery. Appl. Veg. Sci. 13 (2), 221–233 [Online]. https://doi.org/10.1111/j.1654-109X.2009.01063.x.

Hill, R.A., Wilson, A.K., George, M., Hinsley, S.A., 2010. Mapping tree species in temperate deciduous woodland using time-series multi-spectral data. Appl. Veg. Sci. 13 (1), 86–99 [Online]. https://doi.org/10.1111/j.1654-109X.2009.01053.x.

Hubert, M., 2020. 'Robust Methods for High-Dimensional Data'. Comprehensive Chemometrics (Issue June). https://doi.org/10.1016/b978-0-12-409547-2.14883-8.

Hubert, M., Debruyne, M., 2010. Minimum covariance determinant. Wiley Interdiscip. Rev. Comput. Stat. 2 (1), 36–43 [Online]. https://doi.org/10.1002/wics.61.

Hubert, M., Rousseeuw, P.J., Vanden Branden, K., 2005. ROBPCA: a new approach to robust principal component analysis. Technometrics 47 (1), 64–79. https://doi.org/10.1198/004017004000000563.

Imran, H.A., Gianelle, D., Scotton, M., Rocchini, D., Dalponte, M., Macolino, S., Sakowska, K., Pornaro, C., Vescovo, L., 2021. Potential and limitations of grasslands α-diversity prediction using fine-scale hyperspectral imagery. Remote Sens. 13 (14), 1–23 [Online]. https://doi.org/10.3390/rs13142649.

Jacquemoud, S., Baret, F., 1990. PROSPECT: a model of leaf optical properties spectra. Remote Sens. Environ. 34 (2), 75–91 [Online]. https://doi.org/10.1016/0034-4257(90)90100-Z.

Jacquemoud, S., Verhoef, W., Baret, F., Bacour, C., Zarco-Tejada, P.J., Asner, G.P., François, C., Ustin, S.L., 2009. PROSPECT + SAIL models: a review of use for vegetation characterization. Remote Sens. Environ. 113 (Suppl. 1), 56–66. Elsevier Inc. [Online]. https://doi.org/10.1016/j.rse.2008.01.026.

Kokaly, R.F., Despain, D.G., Clark, R.N., Livo, K.E., 2003. Mapping vegetation in Yellowstone National Park using spectral feature analysis of AVIRIS data. Remote Sens. Environ. 84 (3), 437–456 [Online]. https://doi.org/10.1016/S0034-4257(02)00133-5.

LaFleur, B.J., Greevy, R.A., 2009. Introduction to permutation and resampling-based hypothesis tests. J. Clin. Child Adolesc. Psychol. 38 (2), 286–294. https://doi.org/10.1080/15374410902740411.

Lasky, J.R., Uriarte, M., Muscarella, R., 2016. Synchrony, compensatory dynamics, and the functional trait basis of phenological diversity in a tropical dry forest tree community: effects of rainfall seasonality. Environ. Res. Lett. 11 (11) https://doi.org/10.1088/1748-9326/11/11/115003. IOP Publishing. [Online].

Lehnert, L.W., Meyer, H., Obermeier, W.A., Silva, B., Regeling, B., Thies, B., Bendix, J., 2019. Hyperspectral data analysis in R: the hsdar package. J. Stat. Softw. 89 (12), 1–23. https://doi.org/10.18637/jss.v089.i12.

Li, P., Wang, Q., 2011. Retrieval of leaf biochemical parameters using PROSPECT inversion: a new approach for alleviating ill-posed problems. IEEE Trans. Geosci. Remote Sens. 49 (7), 2499–2506. IEEE. [Online]. https://doi.org/10.1109/TGRS.2011.2109390.

Li, Z., Huffman, T., McConkey, B., Townley-Smith, L., 2013. Monitoring and modeling spatial and temporal patterns of grassland dynamics using time-series MODIS NDVI with climate and stocking data. Remote Sens. Environ. 138, 232–244. Elsevier B.V. [Online]. https://doi.org/10.1016/j.rse.2013.07.020.

Lucas, K.L., Carter, G.A., 2008. The use of hyperspectral remote sensing to assess vascular plant species richness on Horn Island, Mississippi. Remote Sens. Environ. 112 (10), 3908–3915 [Online]. https://doi.org/10.1016/j.rse.2008.06.009.

Ma, X., Migliavacca, M., Wirth, C., Bohn, F.J., Huth, A., Richter, R., Mahecha, M.D., 2020. Monitoring plant functional diversity using the reflectance and echo from space. Remote Sens. 12 (8), 1–13 [Online]. https://doi.org/10.3390/RS12081248.

Maclellan, C., 2017. Dual FOV Measurements with SVC HR-1024i Field Spectroradiometers Bi-conical Relative Reflectance Method (Edinburgh, UK).

Magurran, A.E., 2007. Species abundance distributions over time. Ecol. Lett. 10 (5), 347–354. https://doi.org/10.1111/j.1461-0248.2007.01024.x.

Magurran, A.E., McGill, B.J., 2011. Challenges and opportunities in the measurement and assessment of biological diversity. Biol. Divers. Front. Measure Assess. 39–54 [Online]. https://doi.org/10.2307/3547060.

Mazer, S.J., Travers, S.E., Cook, B.I., Jonathan Davies, T., Bolmgren, K., Kraft, N.J.B., Salamin, N., Inouye, D.W., 2013. Flowering date of taxonomic families predicts phenological sensitivity to temperature: implications for forecasting the effects of climate change on unstudied taxa. Am. J. Bot. 100 (7), 1381–1397 [Online]. https://doi.org/10.3732/ajb.1200455.

Mellard, J.P., Audoye, P., Loreau, M., 2019. Seasonal patterns in species diversity across biomes. Ecology 100 (4), 1–15 [Online]. https://doi.org/10.1002/ecy.2627.

Mitchell, D.J., Dujon, A.M., Beckmann, C., Biro, P.A., 2020. Temporal autocorrelation: a neglected factor in the study of behavioral repeatability and plasticity. Behav. Ecol. 31 (1), 222–231 [Online]. https://doi.org/10.1093/beheco/arz180.

Möckel, T., Dalmayne, J., Schmid, B.C., Prentice, H.C., Hall, K., 2016. Airborne hyperspectral data predict fine-scale plant species diversity in grazed dry grasslands. Remote Sens. 8 (2), 1–19 [Online]. https://doi.org/10.3390/rs8020133.

Morellato, L.P.C., Alberton, B., Alvarado, S.T., Borges, B., Buisson, E., Camargo, M.G.G., Cancian, L.F., Carstensen, D.W., Escobar, D.F.E., Leite, P.T.P., Mendoza, I., Rocha, N. M.W.B., Soares, N.C., Silva, T.S.F., Staggemeier, V.G., Streher, A.S., Vargas, B.C., Peres, C.A., 2016. Linking plant phenology to conservation biology. Biol. Conserv. 195, 60–72. https://doi.org/10.1016/j.biocon.2015.12.033.

Morris, E.K., Caruso, T., Buscot, F., Fischer, M., Hancock, C., Maier, T.S., Meiners, T., Müller, C., Obermaier, E., Prati, D., Socher, S.A., Sonnemann, I., Wäschke, N., Wubet, T., Wurst, S., Rillig, M.C., 2014. Choosing and using diversity indices: insights for ecological applications from the German Biodiversity Exploratories. Ecol. Evol. 4 (18), 3514–3524. https://doi.org/10.1002/ece3.1155.

Nakagawa, S., Schielzeth, H., 2013. A general and simple method for obtaining R^2 from generalized linear mixed-effects models. Methods Ecol. Evol. 4 (2), 133–142. https://doi.org/10.1111/j.2041-210x.2012.00261.x.

Nakagawa, S., Johnson, P.C.D., Schielzeth, H., 2017. The coefficient of determination R2 and intra-class correlation coefficient from generalized linear mixed-effects models revisited and expanded. J. R. Soc. Interface 14 (134). https://doi.org/10.1098/rsif.2017.0213 [Online].

Newstrom, L.E., Frankie, G.W., Baker, H.G., 1994. A new classification for plant phenology based on flowering patterns in lowland tropical rain forest trees at La Selva, Costa Rica. Biotropica 26 (2), 141 [Online]. https://doi.org/10.2307/2388804.

Noda, H.M., Muraoka, H., Nasahara, K.N., 2021. Plant ecophysiological processes in spectral profiles: perspective from a deciduous broadleaf forest. J. Plant Res. 134 (4), 737–751. Springer Singapore. [Online]. https://doi.org/10.1007/s10265-021-01302-7.

Ollinger, S.V., 2011. Sources of variability in canopy reflectance and the convergent properties of plants. New Phytol. 189 (2), 375–394. https://doi.org/10.1111/j.1469-8137.2010.03536.x.

Palmer, M.W., Earls, P.G., Hoagland, B.W., White, P.S., Wohlgemuth, T., 2002. Quantitative tools for perfecting species lists. Environmetrics 13 (2). https://doi.org/10.1002/env.516 [Online].

Pinheiro, J.C., Bates, D.M., 2000. Mixed Effect Models in S and S-PLUS. Springer.

Polley, H.W., Yang, C., Wilsey, B.J., Fay, P.A., 2019. Spectral heterogeneity predicts local-scale gamma and beta diversity of Mesic grasslands. Remote Sens. 11 (4), 1–15 [Online]. https://doi.org/10.3390/rs11040458.

Pulungan, M.A., Suzuki, S., Gavina, M.K.A., Tubay, J.M., Ito, H., Nii, M., Ichinose, G., Okabe, T., Ishida, A., Shiyomi, M., Togashi, T., Yoshimura, J., Morita, S., 2019. Grazing enhances species diversity in grassland communities. Sci. Rep. 9 (1), 11201. Springer US. [Online]. https://doi.org/10.1038/s41598-019-47635-1.

Punalekar, S.M., Verhoef, A., Quaife, T.L., Humphries, D., Bermingham, L., Reynolds, C. K., 2018. Application of Sentinel-2A data for pasture biomass monitoring using a physically based radiative transfer model. Remote Sens. Environ. 218, 207–220. https://doi.org/10.1016/j.rse.2018.09.028.

R Core Team, 2021. R: A Language and Environment for Statistical Computing. R Foundation for Statistical Computing, Vienna, Austria. URL. https://www.R-project.org/.

Ramos, D.M., Diniz, P., Valls, J.F.M., 2014. Habitat filtering and interspecific competition influence phenological diversity in an assemblage of Neotropical savanna grasses. Rev. Bras. Bot. 37 (1), 29–36 [Online]. https://doi.org/10.1007/s40415-013-0044-z.

Rathcke, B., Lacey, E.P., 1985. Phenological patterns of terrestrial plants. Annu. Rev. Ecol. Syst. 16 (1985), 179–214.

Rocchini, D., Butini, S.A., Chiarucci, A., 2005. Maximizing plant species inventory efficiency by means of remotely sensed spectral distances. Glob. Ecol. Biogeogr. 14 (5), 431–437 [Online]. https://doi.org/10.1111/j.1466-822x.2005.00169.x.

Rocchini, D., Balkenhol, N., Carter, G.A., Foody, G.M., Gillespie, T.W., He, K.S., Kark, S., Levin, N., Lucas, K., Luoto, M., Nagendra, H., Oldeland, J., Ricotta, C., Southworth, J., Neteler, M., 2010. Remotely sensed spectral heterogeneity as a proxy of species diversity: recent advances and open challenges. Ecol. Inform. 5 (5), 318–329. Elsevier B.V. [Online]. https://doi.org/10.1016/j.ecoinf.2010.06.001.

Schmidt, K.S., Skidmore, A.K., 2003. Spectral discrimination of vegetation types in a coastal wetland. Remote Sens. Environ. 85 (1), 92–108 [Online]. https://doi.org/10.1016/S0034-4257(02)00196-7.

Schmidtlein, S., Fassnacht, F.E., 2017. The spectral variability hypothesis does not hold across landscapes. Remote Sens. Environ. 192, 114–125. Elsevier Inc. [Online]. https://doi.org/10.1016/j.rse.2017.01.036.

Schweiger, A.K., Cavender-Bares, J., Townsend, P.A., Hobbie, S.E., Madritch, M.D., Wang, R., Tilman, D., Gamon, J.A., 2018. Plant spectral diversity integrates functional and phylogenetic components of biodiversity and predicts ecosystem function. Nat. Ecol. Evol. 2 (6), 976–982. https://doi.org/10.1038/s41559-018-0551-1.

Silvertown, J., Poulton, P., Johnston, E., Edwards, G., Heard, M., Biss, P.M., 2006. The park grass experiment 1856-2006: its contribution to ecology. J. Ecol. 94 (4), 801–814 [Online]. https://doi.org/10.1111/j.1365-2745.2006.01145.x.

Smith, B., Wilson, J.B., 1996. A consumer's guide to evenness indices. Oikos 76 (1), 70–82. http://www.jstor.com/stable/3545749.

Stenzel, S., Fassnacht, F.E., Mack, B., Schmidtlein, S., 2017. Identification of high nature value grassland with remote sensing and minimal field data. Ecol. Indic. 74, 28–38. https://doi.org/10.1016/j.ecolind.2016.11.005.

Stohlgren, T.J., 2006. Measuring Plant Diversity: Lessons from the Field. Oxford University Press. https://doi.org/10.1093/acprof:oso/9780195172331.001.0001.

Tansey, C.J., Hadfield, J.D., Phillimore, A.B., 2017. Estimating the ability of plants to plastically track temperature-mediated shifts in the spring phenological optimum. Glob. Chang. Biol. 23 (8), 3321–3334 [Online]. https://doi.org/10.1111/gcb.13624.

Torresani, M., Rocchini, D., Sonnenschein, R., Zebisch, M., Marcantonio, M., Ricotta, C., Tonon, G., 2019. Estimating tree species diversity from space in an alpine conifer forest: the Rao's Q diversity index meets the spectral variation hypothesis. Ecol. Inform. 52 (February), 26–34. Elsevier. [Online]. https://doi.org/10.1016/j.ecoinf.2019.04.001.

Ustin, S.L., Gamon, J.A., 2010. Tansley review: remote sensing of plant functional types. New Phytol. 186, 795–816 [Online]. https://doi.org/10.1111/j.1469-8137.2010.03284.x.

Ustin, S.L., Gitelson, A.A., Jacquemoud, S., Schaepman, M., Asner, G.P., Gamon, J.A., Zarco-Tejada, P., 2009. Retrieval of foliar information about plant pigment systems from high resolution spectroscopy. Remote Sens. Environ. 113 (Suppl. 1), S67–S77. https://doi.org/10.1016/j.rse.2008.10.019.

Voss, M., Sugumaran, R., 2008. Seasonal effect on tree species classification in an urban environment using hyperspectral data, LiDAR, and an object-oriented approach. Sensors 8 (5), 3020–3036 [Online]. https://doi.org/10.3390/s8053020.

Wachendorf, M., Fricke, T., Möckel, T., 2017. Remote sensing as a tool to assess botanical composition, structure, quantity and quality of temperate grasslands. Grass Forage Sci. 1–14. https://doi.org/10.1111/gfs.12312. April 2017.

Wang, R., Gamon, J.A., 2019. Remote sensing of terrestrial plant biodiversity. Remote Sens. Environ. 231 (May), 111218 https://doi.org/10.1016/j.rse.2019.111218.

Wang, R., Gamon, J.A., Montgomery, R.A., Townsend, P.A., Zygielbaum, A.I., Bitan, K., Tilman, D., Cavender-Bares, J., 2016. Seasonal variation in the NDVI-species richness relationship in a prairie grassland experiment (Cedar Creek). Remote Sens. 8 (2) https://doi.org/10.3390/rs8020128 [Online].

Wang, R., Gamon, J.A., Cavender-Bares, J., Townsend, P.A., Zygielbaum, A.I., 2018. The spatial sensitivity of the spectral diversity-biodiversity relationship: an experimental test in a prairie grassland. Ecol. Appl. 28 (2), 541–556 [Online]. https://doi.org/10.1002/eap.1669.

Wehrens, R., 2011. Chemometrics with R: Multivariate Data Analysis in the Natural Sciences and Life Sciences. Springer.

Wolkovich, E.M., Cook, B.I., Davies, T.J., 2014. Progress towards an interdisciplinary science of plant phenology: building predictions across space, time and species diversity. New Phytol. 201 (4), 1156–1162. https://doi.org/10.1111/nph.12599.

Xiao, Y., Zhao, W., Zhou, D., Gong, H., 2014. Sensitivity analysis of vegetation reflectance to biochemical and biophysical variables at leaf, canopy, and regional scales. IEEE Trans. Geosci. Remote Sens. 52 (7), 4014–4024. IEEE. [Online]. https://doi.org/10.1109/TGRS.2013.2278838.

Zuur, A.F., Ieno, E.N., Walker, N.J., Saveliev, A.A., Smith, G.M., 2009. Mixed Effects Models and Extensions in Ecology with R. Springer. https://doi.org/10.1007/978-0-387-87458-6.